CEOS Intercalibration of Ground-Based Spectrometers and Lidars

Second Progress Report

Overview of Scientific Results

Version 1.1
February 2012

DOCUMENT PROPERTIES

Title	CEOS Intercalibration of Ground-Based Spectrometers and Lidars: First Progress Report
Reference	CEOS-IC-PR02
Issue	1.1
Revision	04
Status	Final
Date of issue	28/02/2012
Document type	Report

	FUNCTION	NAME	DATE	SIGNATURE
LEAD AUTHOR	Project coordinator	M. Van Roozendael	15/02/2012	
CONTRIBUTING AUTHORS	Team Leaders	Ulf Köhler Gelsomina Pappalardo Esko Kyrö Alberto Redondas Folkard Wittrock Aldo Amodeo Gaia Pinardi		
REVIEWED BY				
ISSUED BY	Project coordinator	M. Van Roozendael		

DOCUMENT CHANGE RECORD

Issue	Revision	Date	Modified items	Observations
0.0	00	Nov. 2011	Template extracted from PRO01	Creation of document
0.1	01	15/02/2012	First draft version	CINDI NO_2 part missing
0.2	02	24/02/2012	Draft of complete version	For internal review by the team
1.0	03	27/02/2012	Complete version	Waiting corrections
1.1	04	28/02/2012	Final version delivered to ESA	

Table of Content

Table of Figures

1 Executive summary

This document summarizes activities and achievements during the second part of the ESA CEOS Intercalibration project. The period covered by this report extends from February 2011 until January 2012.

Dobson activities

As part of the activities of the Regional Dobson Calibration Center for Europe (RDCC-E) three campaigns were organized, two of them funded by this project, one as a regular Dobson intercomparison on the DWD RDCC-budget: Nordic Campaign 2011 ("SAUNA III"), El Areno 2011 (both funded by ESA) and MOHp 2011 (DWD funding). In addition the RDCC-E representative participated in the WMO/UNEP Dobson Data Quality Workshop, organized by the RDCC partner Solar and Ozone Observatory in Hradec Kralove, SOO-HK, Czech Republic). An intense training course became necessary for the successor of the retired Dobson technician. Two Dobsons were completely refurbished and electronically upgraded as part of the capacity building task.

Brewer activities

Three campaigns with the participation of the RBCC-E and two of FMI were organized with the support of this project: Sodankylä 2011, Arenosillo 2011 and Izaña 2011. During the standard intercomparison campaign at El Arenosillo the calibration of the reference triad was transferred to the participating instruments and comparison were performed with the Dobson European Standard of RDCC_E. The campaigns at Sodankylä and Izaña were specific for this project. Both Sodankylä 2011 and Izaña 2011, with the participation of brewers #037 and #107, tried to determine how the calibration transfer was affected by the atmospheric conditions, comparing the calibration at Izaña (Subtropical) to the calibration performed on site (Artic). The participation of the Dobson Standard at Huelva and Sondankyla allows also the Brewer-Dobson comparison at high ozone slant path (Sondankyla) and low ozone slant path conditions (Huelva).

Important advances have been achieved in the calibration procedure, and a summary calibration checklist has been adopted. The use of this checklist allows data users to perform a quick diagnosis of the calibration of any particular instrument. In addition two issues that affect the instrumental calibration have been identified and the corresponding effects have been analyzed: non linearity of the attenuation filter and errors related to the Dead Time correction.

UV-Vis MAXDOAS activities

During this part of the project, activities concentrated on the post-campaign exploitation of the data. Following the NO_2 and O_4 slant column intercomparison published in AMT in 2010, a similar exercise was undertaken for the more challenging formaldehyde (HCHO) measurements. After harmonization of the DOAS retrieval settings, HCHO slant column derived from 9 different instruments were found to agree within plus or minus 15 percent despite the large variety of the

instrumental designs involved. In a second part of the same study, the sources of systematic uncertainties were investigated by means of a sensitivity analysis on the fitting parameters and retrieval settings. Results indicate that systematic uncertainties are in the range of 20 to 40 percent depending on the solar zenith angle.

In parallel to the HCHO study, the MAXDOAS NO_2 profile intercomparison has been continued, with a major focus on studying the stability of various retrieval schemes under a variety of simulated atmospheric conditions. This work is preparatory for future algorithm haramonization. It has been shown that for the most important parameters, i.e. the tropospheric vertical column and the mixing ratio close to the surface – the different MAX-DOAS methods are able to reproduce the truth within 25% even for higher aerosol (AOD=0.54) and more difficult scenarios like uplifted NO_2-layers. The retrieval in the visible (at 477 nm) is generally more stable and results are closer to reality than in the UV (at 360 nm) which is mainly due to the lower impact of aerosols. Finally it was found that even with a simple geometric approach it is possible to identify in average the right number for the tropospheric column, although with larger noise and limitations on the possible geometries of the measurements.

EARLINET calibration activities

Five intercomparison measurement campaigns were carried out in 2009 and 2010: EARLI09, ALI09, SOLI10, ROLI10 and SPALI10. The intercomparison measurement campaigns allowed to compare the performances of many lidar systems, to define a standard methodology to be applied in the lidar system intercomparison, to confirm the possibility to obtain reliable and homogeneous data within EARLINET, but also to understand the reasons of the possible failures and to individuate the way to solve them.

2 Introduction

2.1 Scope of this document

This document is the second progress report of the CEOS Intercalibration of Ground-Based Spectrometers and Lidars project. It summarizes activities performed and results achieved within each team during the period from March until December 2011.

2.2 Acronyms and abbreviations

ACSG	Atmospheric Composition Subgroup of the CEOS-WGCV
BAS	British Antarctic Survey
BIRA-IASB	Belgian Institute for Space Aeronomy
Cal/Val	Calibration and Validation
CEOS	Committee on Earth Observation Satellites
CNR-IMAA	Consiglio Nazionale delle Ricerche- Istituto di Metodologie per l'Analisi Ambientale
CNRS-SA	Service d'Aéronomie du CNRS
DMB	Daumont – Malicet – Brion (new ozone absorption coefficients)
DOAS	Differential Optical Absorption Spectroscopy
DWD	Deutscher Wetterdienst (German National Meteorological Service)
EARLINET	European Aerosol Research Lidar Network
EARLINET-ASOS	European Aerosol Research Lidar Network - Advanced Sustainable Observation System
ENVISAT	Environmental Satellite
EO	Earth Observation
EOS	(NASA's) Earth Observing System
ERS-2	European Remote Sensing Satellite-2
ESA	European Space Agency
ESRIN	European Space Research Institute
EUMETSAT	European Organisation for the Exploitation of Meteorological Satellites
FFT	Fast Fourier Transform
FP7	Seventh Framework Preogramme of the European Commission
FTIR	Fourier Transform Infrared Radiometer
GAW	Global Atmospheric Watch
GEO	Geostationary orbit
GEOSS	Global Earth Observation System of Systems
GMES	Global Monitoring of Environment and Security
GOME	Global Ozone Monitoring Experiment
IGACO	Integrated Global Atmospheric Chemistry Observations IGOS Theme
IGOS	The Integrated Global Observing Strategy
INTA	Instituto Nacional de Técnica Aeroespacial
IUP	Institute of Environmental Physics
KNMI	Royal Netherlands Meteorological Institute
MAXDOAS	Multi-Axis DOAS

METOP	Meteorological Operational satellite programme
MOHp	Meteorological Observatory Hohenpeissenberg
MPI	Max-Planck-Institute
NASA	National Aeronautics and Space Administration
NDACC	Network for the Detection of Atmospheric Composition Change
OMI	Ozone Monitoring Instrument
QA	Quality Assessment
RDCC-E	Regional Dobson Calibration Centre for Europe
RT	Radiative Transfer
SCIAMACHY	SCanning Imaging Absorption spectroMeter for Atmospheric CartograpHY
SOO-HK	Solar and Ozone Observatory Hradec Kralove
SOW	Statement of Work
SZA	Solar Zenith Angle
TOMS	Total Ozone Mapping Spectrometer
WCWG	CEOS Working Group on Calibration and Validation
WDCC	World Dobson Calibration Centre
WMO	World Meteorological Office
WPDS	World Primary Dobson Spectrophotometer D083
WOUDC	World Ozone and Ultraviolet Data Center

2.3 Applicable documents

[AD1] CEOS Intercalibration of Ground-Based Spectrometers and Lidars, Proposal in response to ESRIN/RFQ/3-12340/08/I-EC (ref. this proposal).

[AD2] ESA/ESRIN Statement of Work, ref. SOW: CEOS Intercalibration of ground-based spectrometers and lidars, GMES-CLVL-EOPG-SW-08-0002.

[AD3] Draft Contract, Appendix 2 to ESRIN/RFQ/3-12340/08/I-EC

2.4 Reference Documents

[RD1] Vicarious Calibration and Geophysical Validation Functional Baseline, GMES-SPPA-EOPG-TN-06-0001.

[RD2] ENVISAT Calibration and Validation Plan, PO-PL-ESA-GS-1092.

[RD3] IGOS – Integrated Global Observing Strategy: Atmospheric Chemistry, http://ioc.unesco.org/igodpartners/atmosphere.htm

[RD4] CEOS – Working Group on Calibration and Validation: Satellite missions/ Atmospheric Chemistry, http://www.oma.be/NDSC_SatWG/Documents/SatelliteMissionsPlanning(30 Nov2007)_A4.pdf

3 Work in progress

This chapter describes the activities having taken place during the first contractual part of the project. Main results obtained in each team are highlighted.

3.1 Dobson and Brewer calibration activities

3.1.1 Activities of the Regional Dobson Calibration Center for Europe (RDCC-E) at Meteorological Observatory Hohenpeissenberg (MOHp)

In the second phase of the project two campaigns were performed, which were funded by ESA; one campaign was organized as official WMO RDCC-E intercomparison under the auspices of and funding by DWD:

- Nordic Campaign 2011 (Sodankylä, Finland, March 7 – 25) – This campaign was a repetition of the two SAUNA campaigns I (March/April 2006) and II (February – April 2007). The European Reference Dobson No. 064 from Hohenpeissenberg participated only in SAUNA I. In 2011 in addition to D064 the Swedish Dobson No. 030 took part, which was just refurbished and calibrated towards D064 during MOHp2010 eight months before.

- ElAreno 2011 (Spain, July 4 to 15) was again a combined campaign for calibration of Dobsons in the European network (4 Dobsons from Iceland, France, Spain and Italy) and for comparison of the reference Dobson and Brewer in Europe. The results of a similar campaign in 2009 should be compared and hopefully confirmed.

- MOHp 2011 was conducted from August 29 to September 16. Three Dobsons from Egypt (completely refurbished before), United Kingdom and Romania were undergone a regular calibration service. This activity was funded by DWD.

Another important activity was the participation in the WMO/UNEP Dobson Data Quality Workshop, organized by the RDCC-E partner Solar and Ozone Observatory in Hradec Kralove (SOO-HK) in Czech Republic from February 14 to 18. Main goal of this meeting was to bring together on the one hand Dobson experts and on the other hand data producers and data users (e.g. satellite scientists) to exchange experiences and to transfer the necessary knowledge, how to examine, to assess and to reprocess long term data records.

A not expected activity became necessary, when the Dobson technician Bert Dömling retired in March 2011 and the designated successor Michael Heinen could not start his new job before November 2011. Without overlap and training by Bert Dömling a special training course was organized during two weeks in November. This course was held by the Czech Dobson and Brewer expert Martin Stanek from SOO-HK and funded through the visiting scientist budget of the DWD.

Two Dobsons have got an electronical, optical and mechanical upgrading.The Egyptian Dobson No. 096 was completely refurbished in the run-up of MOHp 2011. Now all three Egyptian Dobsons are upgraded and build an important part in the African network of monitoring the ozone layer. The

decommissioned D014 from Tromsoe (loan of the International Ozone Commission IO_3C to Norway) was used as training object during the course for Michael Heinen. It will be available for relocation to fill gaps in the global network after final calibration in spring/summer 2012.

Results of the Nordic Campaign 2011

Main objective of this campaign was to compare the data quality of the Dobson spectrometer type with the modern Brewer instrument under extreme conditions. This means on the one hand observations at cold ambient temperatures and on the other hand at low sun and normally high total ozone columns (TOC). The Swedish Dobson No. 030 participated in this campaign too. As this instrument was calibrated in summer 2010, it was interesting to investigate the agreement or discrepancy between both Dobsons under normal conditions during a calibration campaign at Hohenpeissenberg and during the extrem conditions at Sodankylä.

First of all it could be stated, that both Dobsons and even their operators withstood the cold temperatures down to -20^o C in the morning of each measurement day. However, it was noticed, that too rapid instrumental temperature changes affected the correct setting of the wavelengths. It was found by means of several mercury lamp tests (HG-tests) that the applied so-called Q-tables were temporarily not correct, when the Dobsons were moved outdoors from the relatively warm shelter. Then the optical parts were not in a thermal balance until the speed of temperature change became normal.

Special investigations at Hohenpeissenberg during the refurbishment of D014 showed this feature:
The results of the test to derive the temperature coefficients of the refurbished Dobson No. 014 strongly depend on the speed of the change of the intrumental temperature. Thermal imbalance of the optics causes hysteresis effects and yield totally different temperature coefficients (Figure 1).

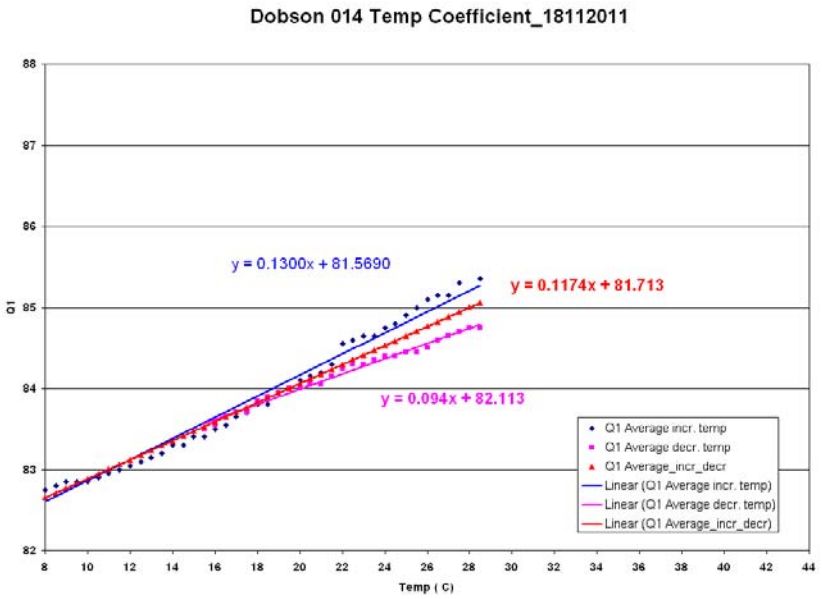

Figure 1: Large differences in the temperature coefficients for Dobson No. 014 during tests with rapidly increasing and decreasing temperatures.

Another test over two days with slowly changed temperatures provide much more consistent results and a temperature coefficient, which significantly differs from that on the day with rapid temperature changes (Figure 2).

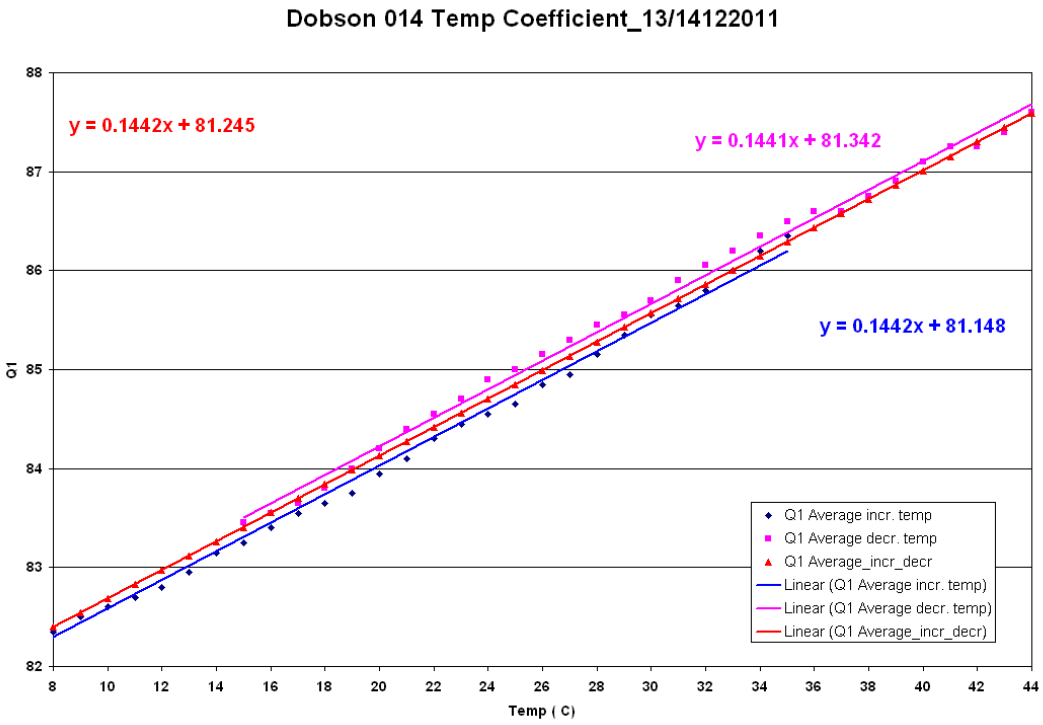

Figure 2: Temperature coefficients for Dobson No. 014 during tests with slowly increasing and decreasing temperatures.

This effect can possibly explain why the results of both Dobsons No. 030 and 064 on the first day (March 13, 2011) of comparative measurements look a little bit odd. The CD-values were permanently lower than the AD-data, even at very low sun (Figure 3). This is normally not the case during regular observations under normal conditions.

After realisation of this problem, the Q-tables of both Dobsons were improved applying more frequent HG-tests during the phase with rapidly increasing temperature. This improvement clearly results in a normal behaviour, that means CD-data are higher than AD at Mu-values which are at least larger than 3.5. This can be seen in Figure 4 with the data on March 16.

An additional, very interesting result is the rather good agreement of the focussed moon observations with the daily direct sun data. Although it was only a little bit more than a half moon, the averages of the night data of both Dobsons are very close to the daily mean. It should be mentioned, that this type of observations is not done very frequent and normally restricted to stations in high latitudes during winter season, when regular Direct Sun (DS) observations are not possible.

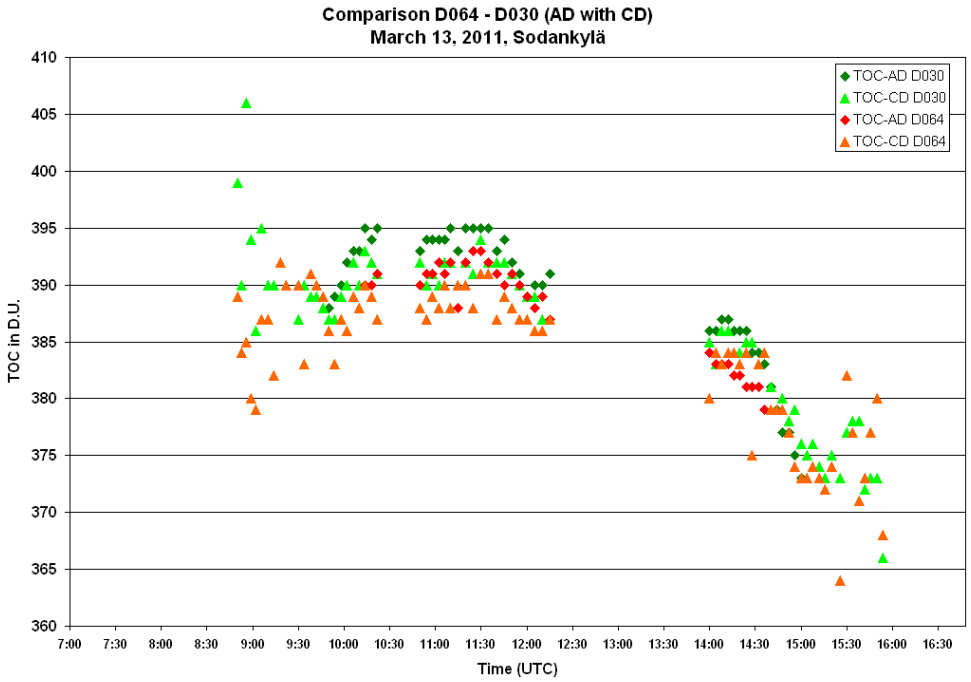

Figure 3: AD- and CD-observations of D030 and D064 on March 13.

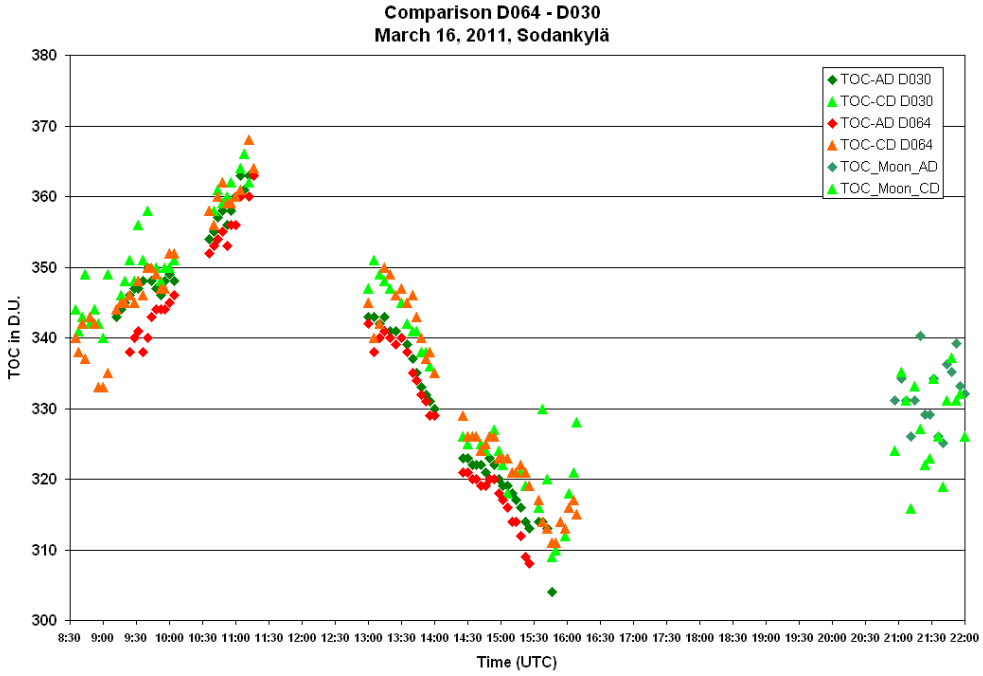

Figure 4: AD- and CD-observations of D030 and D064 on March 16.

The comparison of the reference Dobson No. 064 with the reference Brewer No. 185 (see chapter 3.1.2 by Alberto Redondas) showed the already known results. The difference was rather high with values around – 3 to -4 % depending on wavelength pairs and on sun position. Similar values were observed during the SAUNA I campaign at Sodankylä five years ago.

The main contributions, however, to these large differences are not caused by the instruments' properties themselves like straylight effects, miscalibrations etc.. It can be shown that taking into account on the one hand the different temperature dependencies of the ozone absorption coefficients of the two spectrometer types and on the other hand the differences in the calculation of Mu (Brewer algorithm always takes 22 km as height of the ozone layer, whereas the Dobson algorithm applies a latitudinally depending height, which is 19 km in Finland) the major part of the differences can be explained and corrected (see Figure 5). The original Dobson data (Dobsons No. 030 light blue diamonds and 064 magenta squares) on March 16 are close together, but about 4 % lower than the Brewer values. The temperature corrected D064-data incl. Mu-calculation according the Brewer algorithm (red squares) fit much better. Another significant improvement is to use CD-data instead of AD, which is normally recommended in the Dobson SOP's at Mu-values above 3.5. The D064-values (blue squares) are now very close to the Brewer No. 185 data and mostly within the ± 1%-limit.

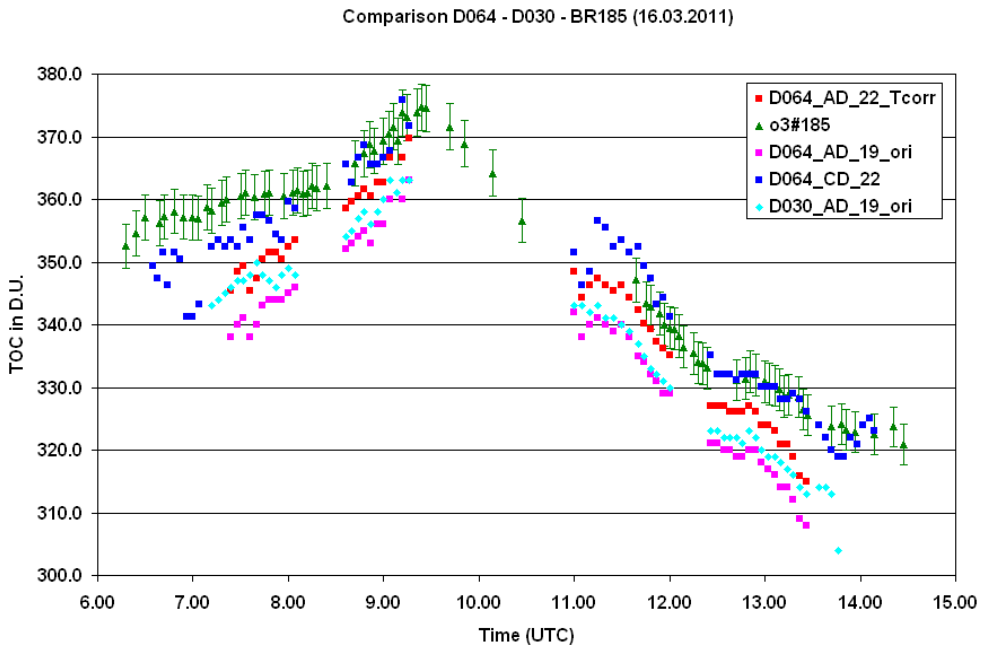

Figure 5: AD- and CD-observations of D030 and D064without and with corrections in comparison with Brewer No. 185 on March 16, 2011.

Results of Dobson-Brewer comparison ElAreno 2011

The second Spanish Dobson-Brewer intercomparison campaign in this ESA CEOS project after 2009 took place from July 4 to 15, 2011.

The 2009 results with average differences between reference Dobson and Brewers within about 1% and a daily course with the biggest difference at noon are confirmed. One example of July 6, 2011 (Figure 6), is representative for all other days with intercomparison measurements. The interesting pattern, found in 2009, that the Brewer data showed a symmetrical course with higher values at noon, whereas the Dobson D064-data were rather constant, cannot be seen so clearly in 2011.

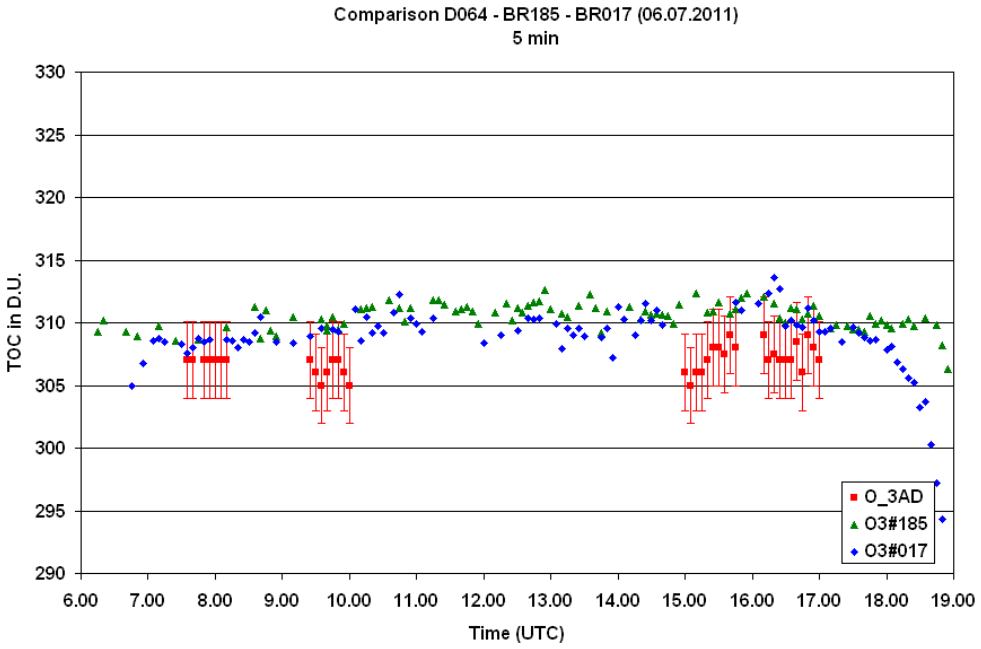

Figure 6: Comparison of Dobson No. 064, Brewer No.'s 17 and 185 on July 6, 2011.

The principal difference of about 1% between Dobson and Brewer reference instruments obviously comes from a slightly different calibration level, as it could be observed during other campaigns like the Brewer No. 010 – calibration in May 2011 too (Figure 7). After correction of the temperature dependency by an increase of 0.46% (effective temperature of the ozone layer was -49.9^{o} C instead of -46.3^{o} C) the D064-data (original data as orange squares, corrected red diamonds) are again mostly within the ± 1%-limit.

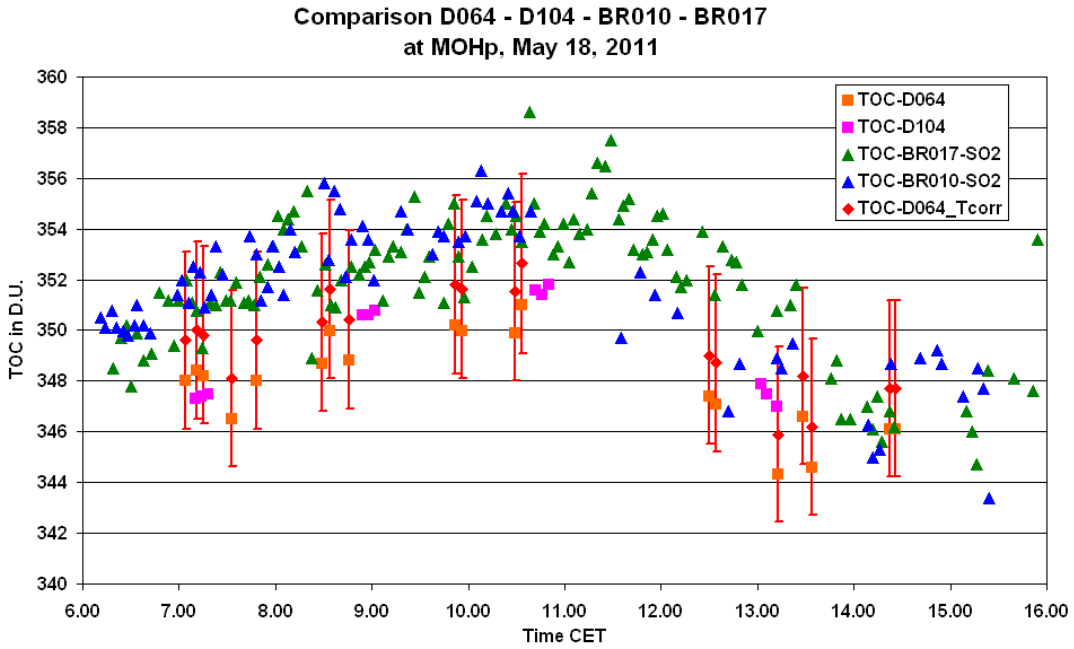

Figure 7: Comparison of Dobson No. 064, Dobson No. 104, Brewer No.'s 010 and 017 on May 18, 2011 at MOHp.

Results of Dobson comparisons ElAreno2011 and MOHp 2011

In Spain four Dobsons (No. 048 from Italy, No. 50 from Iceland, No. 085 from France and No. 120 from Spain) were checked and successfully calibrated against the reference Dobson No. 064 from Hohenpeissenberg.

The main goals of MOHp2011 were the refurbishment of the Egyptian Dobson No. 096 and the calibration service of this instrument, the UK-Dobson No. 032 and the Romanian No. 121.

Figure 8 shows the very good agreement of all Dobsons during the initial comparisons at both campaigns, before any work was done with the instruments. As contrast to the European campaigns the results of the South America intercomparison in 2010 show a certain number of Dobsons which do not match the ± 1%-limit. This reflects the fact, that the RDCC-E has been in operation now for more than ten years and most of the European Dobsons have got at least one regulare calibration service, whereas the RDCC South America has been just established.

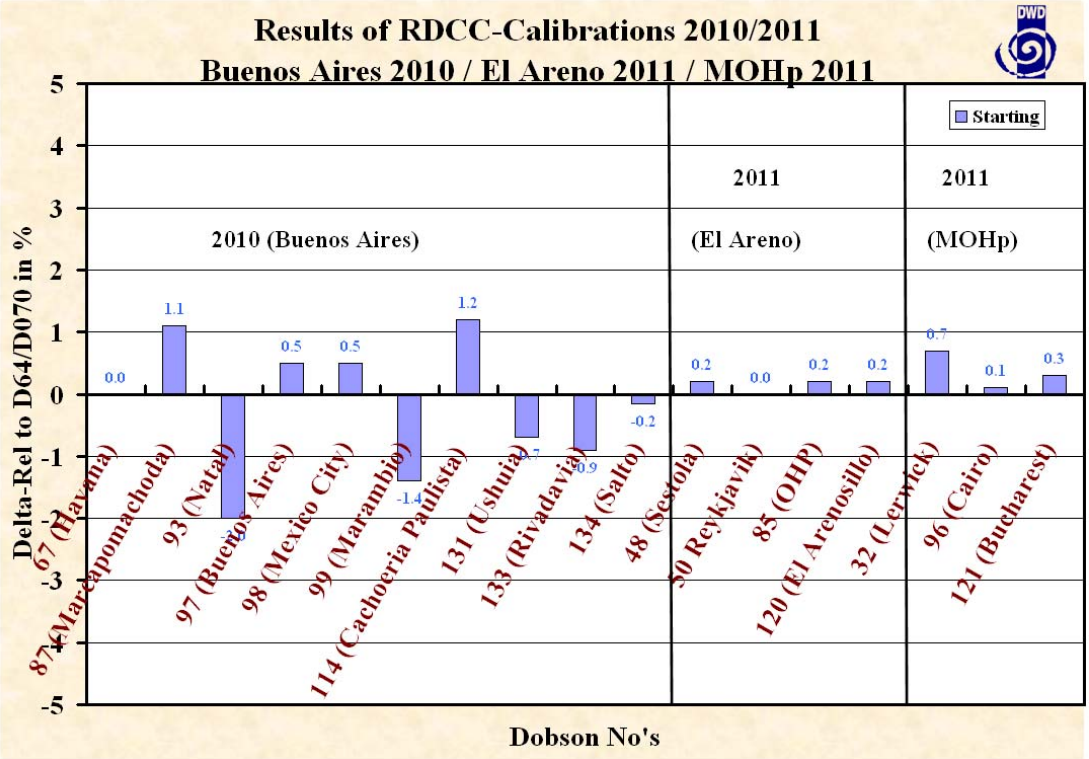

Figure 8: Initial calibration of the European field Dobsons during the RDCC-E campaigns of the past year and the South America Dobsons in 2010.

Results of other activities

The investigations of straylight effects inside the Dobson and the measurements of the individual slith widths of each instrument became less important for the present for several reasons:

- Replacement of the RDCC-E "Dobson-expert" Bert Dömling, therefore at first necessary training of his successor Michael Heinen.
- Measurements of slit widths with a special device revealed problems at some Dobsons. As the photomultiplier tube (PMT) has to be replaced during this procedure by a mini-UV-spectrometer, not all Dobsons came back to their original calibration status. The position of the reinstalled PMT was changed a little bit and had to be adjusted.
- The most important issue is currently the introduction of the new ozone cross sections/absorption coefficients. The subsequently necessary reprocessing of the Dobson and Brewer data incl. re-evaluation of their differences absolute priority. It does not make sense to continue other work or even to start new activities before this action will have been finished. It is hoped, that the new Daumont-Malicet-Brion (DMB) coefficients will replace the old Bass-Paur (BP) coefficients within the coming year.

3.1.2 Activities of the Regional Brewer Calibration Center for Europe (RBCC-E) at Izana and Nordic Brewer campaing activities (FMI)

3.1.2.1 Reference calibration and Stability between travels

The Regional Brewer Calibration Center for Europe (RBCC-E) was established at the Izaña Atmospheric Research Centre in 2003. The RBCC-E transfers the calibration from the world reference triad located in Toronto (Canada) and managed by the EC-MSC (Environmental Canada, Meteorological Service of Canada). The link of the world triad is performed yearly through the travelling Brewer #017, managed by the private company IOS (International Ozone Services) until now. For the forthcoming years the technical maintenance of the instruments will be performed by Kipp & Zonen, brewer manufacturer, and the link will be directly with the world triad in Toronto or by common Langley campaigns at Mauna Loa or IZO.

Preliminary results of the campaigns on this reporting period show that the RBCC-E reference is about 1% over the "mean" of brewer in Sodankyla and also 1% higher than the Dobson reference in Huelva. The efforts have been directed at RBCC_E to ensure the calibration of the triad and the stability of the traveling reference before and after the campaign. These efforts have intensified due to the actual situation of Environmental Canada and doubts about the future of the world reference triad. In the last WMO SAG ozone meeting, RBCC-E was allowed to transfer his own calibration based on Langley at Izaña Atmospheric Observatory (IZO).

To assure the calibration of the triad, a routine calibration is performed every week at IZO and the frequency of the instrumental tests like wavelength calibration were increased from yearly basis to monthly. The measurement schedule has been adapted to maximize the Langley observations reducing the spectral UV and Umkher measurement program.

The last "world travelling reference triad to European reference triad" calibration transfer was performed in July 2011 but we have not received the results. For this report we use the calibration performed in September 2010. The comparison of the triad with the IOS travelling reference Brewer #017 at Izaña during the period September 20–27, 2010 is shown in Figure 9 and summarized in Table 1.

.

Summary of results: IOS calibration 2010	#157	#183	#185
SL ratios 2010 – final	350/590	335/600	311/450
ETC constants 2010	1605/180	1596/220	1574/80
Cal step	1026	1023	284
Absorption Coeff's.	0.3397/1.15	0.3415/1.146	0.3422/1.15

Table 1: Summary of calibration constants after IOS 2010, Izaña

The stability of the travelling standard is checked before and after the campaign, by comparison with the other instruments of the triad, and if possible by performing a Langley analysis. Figure 10 shows the ratio of simultaneous measurements of the RBCC-E Brewer triad for a period of 10 days before (February 21 – 28, 2011) and after (April 1 – 10, 2011) Sodankyla 2011campaign. Note that the reference is the mean of all three instruments (Brewers #157, #183 and #185). One can observe an

excellent agreement between Brewer #157 and #185, within 0.5%, whereas the maximum relative differences correspond to Brewer #183 but these results are also stable before and after the travel.

The same results are obtained before and after Huelva (summarized in Table 2). In addition, a Langley analysis confirms the calibration of the instrument. The figures show the ratio of simultaneous measurements of the Brewer triad for ten days before the campaign. The reference is the mean of brewer #157 and #185.

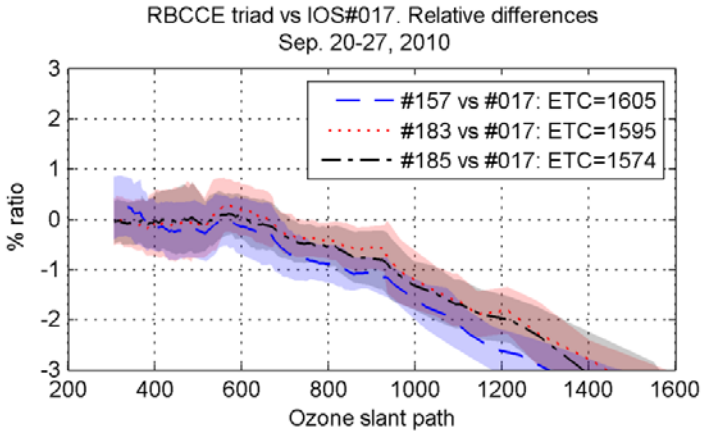

Figure 9: Ratio to the traveling reference #017 of the RBCC-E triad in September 2010

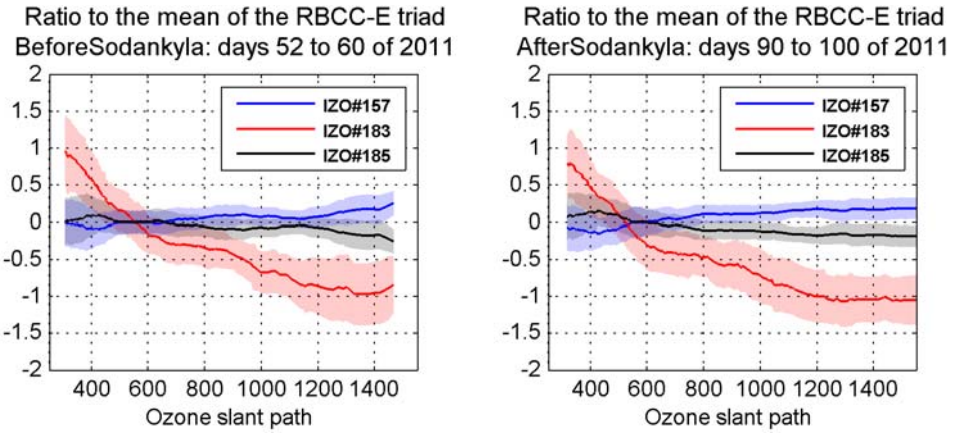

Figure 10: Ratio of simultaneous measurements of RBCC-E standards (Brewers #157, #183 and #185) to the mean of all instruments. Before (left, Julian days 52 to 60) and after (right, Julian days 90 to 100) Sodankylä intercomparison.

	#157	#183	#185	Nobs
Before	-0.07 +/-0.34	-0.22 +/-0.40	0.07 +/-0.34	390
After	-0.07 +/-0.23	-0.34 +/-0.50	0.07 +/-0.23	75

Table 2: Mean and standard deviation of the Brewer of the triad against the mean of #157 and #185, before and After Huelva campaign

Month	ETC(AM)	Se	Nobs	ETC(PM)	Se	Nobs	ETC	Se	Nobs
April	1581.5	1.5	2	1573.8	4.4	6	1575.7	3.5	8
May	1575.9	3.3	14	1572.5	4.2	6	1574.9	2.6	20
Jun	1573.3	6.1	10	1582.5	3.7	16	1577.1	3.4	28
Total	1575.3	2.9	26	1578.5	2.6	28	1576.1	1.9	56

Table 3: Extra-terrestrial constant calculations for the brewer #185 on period before Huelva campaign monthly: mean, standard error and number of observations for morning Langley (AM), and afternoon (PM) and all the cases.

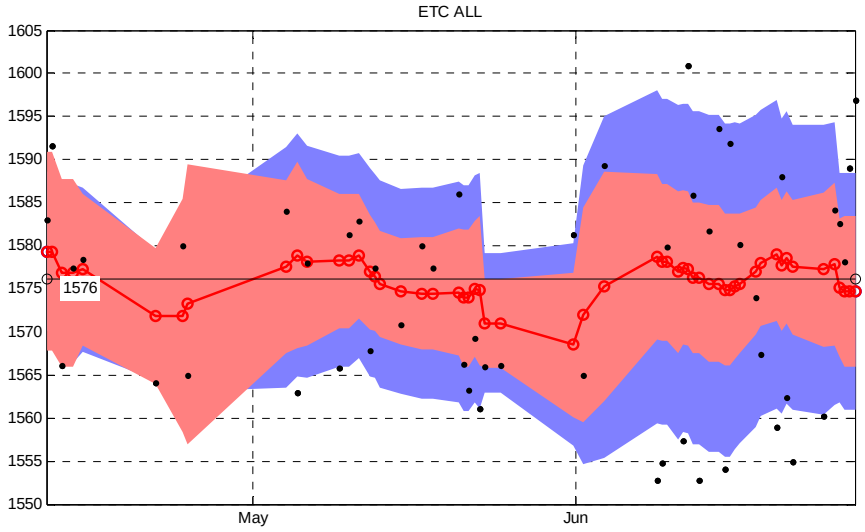

Figure 11: Langley ETC calculations at Izaña Atmospheric observatory before the campaign

After the Huelva campaign the micrometers of Brewer#185 had to be adjusted resulting in a big change on the instrument. The instrument is still changing as demonstrated by the R6 ratios, and until now no optimal calibration could be derived. On the other hand, the update of the "calc-step" in #183 brings this instrument very close to the reference Brewer #157.

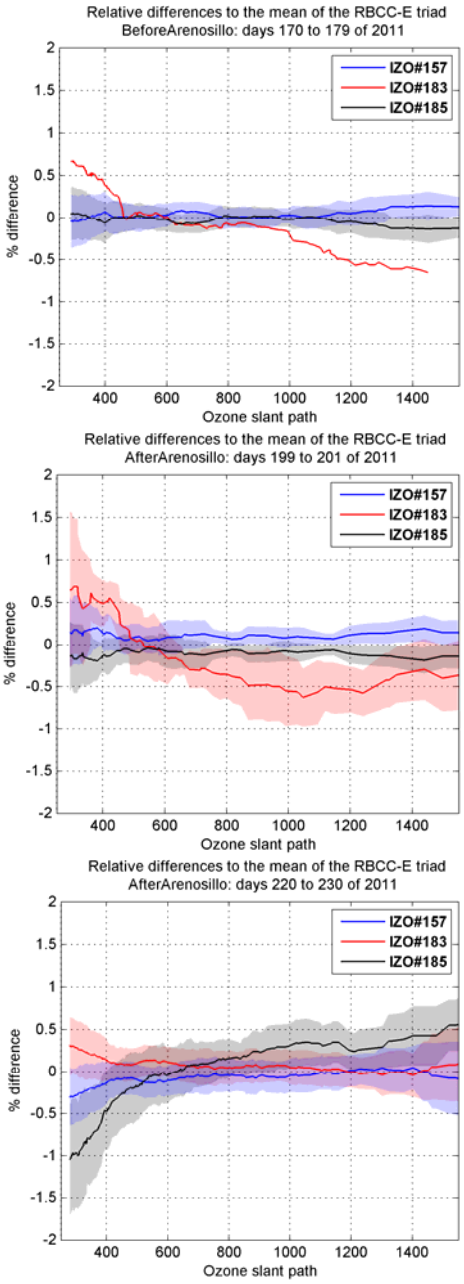

Figure 12: Relative differences Relative differences of simultaneous measurements of RBCC-E standards (Brewers #157, #183 and #185) to mean of all instruments. Before (upper , Julian days 170 to 179), after (middle, Julian days 220 to 230) Huelva intercomparison and after IOS maintenance (down, Julian days 220 to 230)

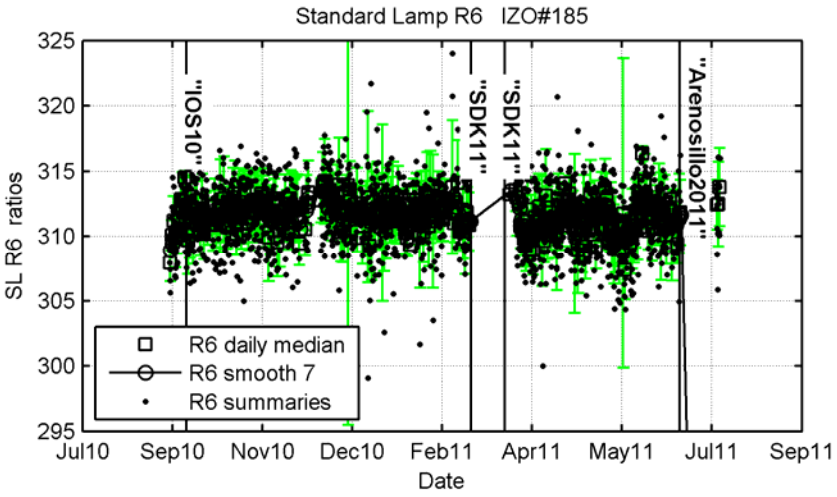

Figure 13: R6 ratios since September 2010

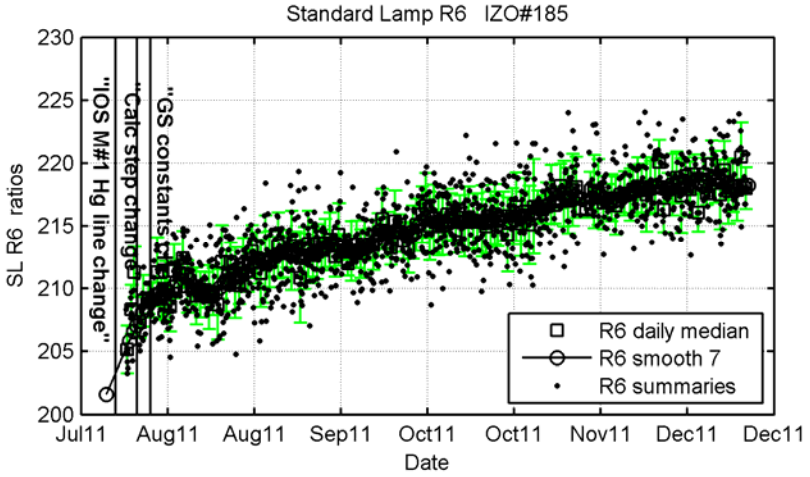

Figure 14: R6 ratios after the maintenance

3.1.2.2 Calibration Campaigns

The Sixth Regional Brewer Calibration Centre for Europe (RBCC-E) intercomparison was held at El Arenosillo Atmospheric Sounding Station of the "Instituto Nacional de Técnica Aeroespacial" (INTA) during the period July 5-15, 2011. This sixth campaign was a joint exercise of the Regional Dobson Calibration Center for Europe (RDCC-E) and the Regional Brewer Calibration Center for Europe (RBCC-E) in collaboration with the Area of Instrumentation and Atmospheric Research of INTA, with the support of the Global Atmospheric Watch (GAW) program of the World Meteorological Organization (WMO) and a CEOS project of the European Space Agency (ESA). At the Arenosillo campaign seventeen brewer instruments participated from seven countries. In addition five Dobson instruments participated in a parallel RDCC-E campaign. The weather conditions were excellent (clear sky conditions on all days), which allowed to reduce the synchronization time to 5 minutes (instead of 10) while taking more than 400 simultaneous measurements.

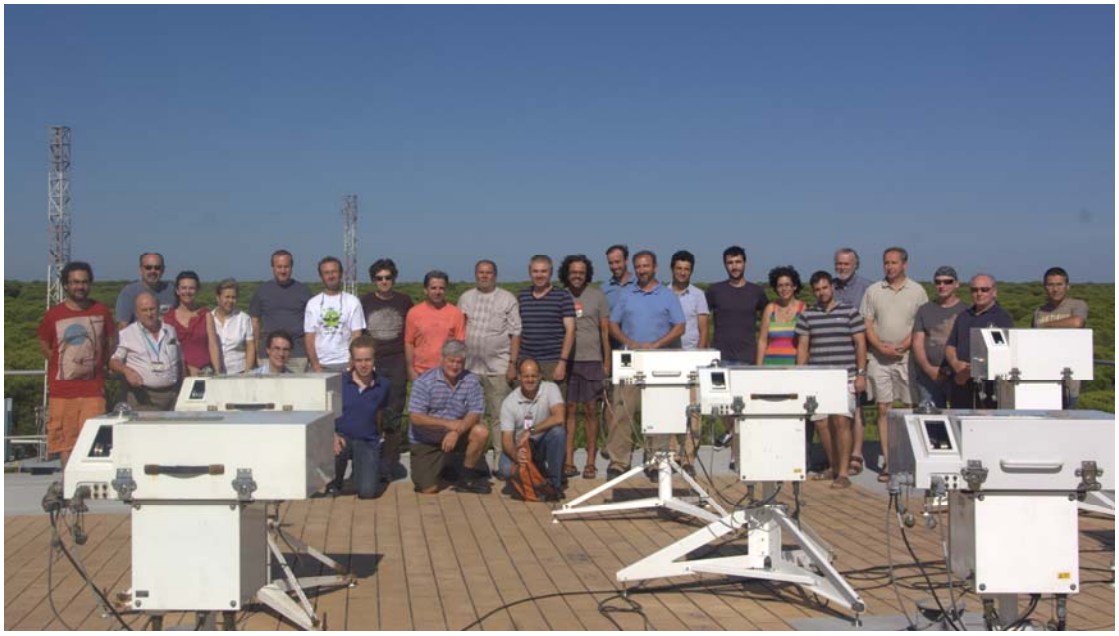

Figure 15: Group photo at the Huelva 2011 campaign

Figure 16. Brewer participating at the Arenosillo 2011 campaign

The results of the 2011 intercomparison are comparable to those of the 2009 campaign. In the blind-comparison, the observations which were processed with the user provided calibration and corrected by Standard Lamp (Fioletov et al., 2005) are quite good. All of the participants with the exception of two not operative brewers are in the range [-1.5-1%], 80% of the instruments are around +/- 1% and two thirds of that show a perfect agreement of +/- 0.5%. The campaign is almost processed and the individual reports are in correction process.

Institution	Name	Brewer/Dobson	Country
IOS	Ken Lamb Martin Stanek	Brewer #017-MKII	Canada Czech Republic
INTA Huelva	J. Ml Vilaplana	Brewer #150-MKIII	Spain
RBCC-E AEMET	Alberto Redondas Juan José Rodriguez Virgilio Carreño	Brewer #185-MKIII	Spain
DMN	Zaidouni Taoufik Amrhar Hassan Zaydi Mustapha J. E. Mohammed	Brewer #051-MKII Brewer#165 - MKIII	Morroco
AEMET	María Lopez Jose Montero J.M Anastasio Jose Antonio Parodi Francisco García	Brewer #070-MKIV Brewer #186-MKIII Brewer #166-MKIV Brewer #117-MKIV Brewer #151-MKIV	Spain
UKMO	John Rimmer Peter Kelly	Brewer #075-MKIV Brewer #126-MKII Brewer #172-MKIII	U.K.
WRC	Gregor Hülsen	Brewer #163-MKIII QUASUME	Switzerland
K&Z	Arjan Hoogendoorn	Brewer #158-MKIII Brewer #201-MKIII	Netherland
MSC	Tom McElroy V. Savastiouk	Brewer #145-MKIII	Canada

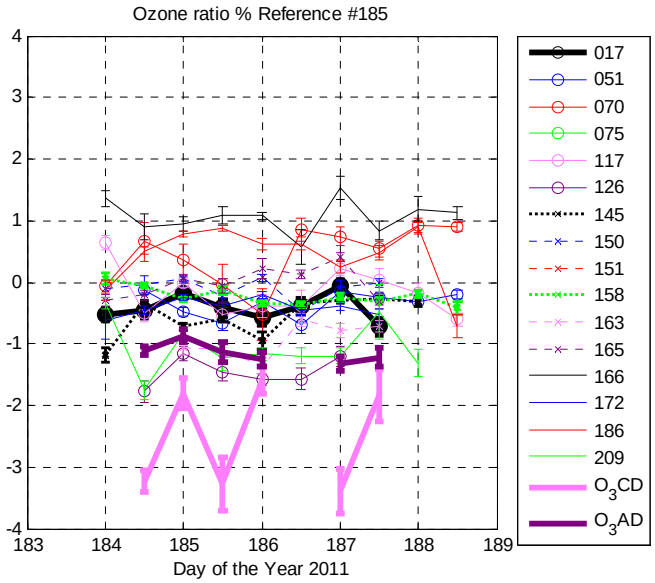

Figure 17: Daily mean of the simultaneous ozone observations at Arenosillo 2011 campaign, initial configuration of the brewer are used. (Reference brewers are marked with thicker lines)

	186	187	188	189	190	191	192	193	194	195	avg.	std.	Obs.
17	**-0.5**	**-0.5**	**-0.2**	**-0.4**	**-0.6**	**-0.4**	**-0.1**	**-0.7**	**-1.9**		**-0.4**	**0.1**	**431**
51		-0.1	-0.5	-0.7	-0.3	-0.7	-0.1	-0.2	-0.3	-0.2	-0.4	0.1	424
70	-0.1	0.7	0.4	0	-0.5	0.9	0.7	0.5	0.9	0.9	0.4	0.2	307
75	-20	-23	18	23	19	23	23	20			10.	1.4	275
117	0.6	-0.5	0	-0.5	-0.4	-0.4	0.2	0	-0.2	-0.6	-0.2	0.2	463
126	-1.3	-1.8	-1.2	-1.5	-1.6	-1.6	-1.2	-1.2			-1.5	0.2	201
145	**-1.2**	**-0.3**	**-0.7**	**-0.6**	**-0.9**	**-0.3**	**-0.3**	**-0.3**	**-0.3**		**-0.6**	**0.1**	**442**
150	-0.1	0	0	-0.2	0.1	-0.5	-0.1	0	-0.2	0	-0.1	0.1	344
151	-32	-33	-31	-31	-21	-25	-30	-27	-30	-33	-29	1.2	387
158	**0.1**	**0**	**-0.3**	**-0.1**	**-0.3**	**-0.4**	**-0.2**	**-0.3**	**-0.2**	**-0.4**	**-0.2**	**0.1**	**471**
163			-1.1	-1.1	-1.4	-0.6	-0.8	-0.7	-0.2		-0.9	0.1	347
165	-0.3	-0.2	0.1	-0.1	0.2	0.1	0.4	-0.3	-1	-0.1	0	0.1	371
166	1.4	0.9	1	1.1	1.1	0.6	1.5	0.8	1.2	1.1	1.1	0.2	463
172	-0.6	-0.5	-0.2	-0.4	-0.2	-0.5	-0.4	-0.5			-0.4	0.1	395
186	-0.1	0.5	0.8	0.9	0.6	0.6	0.2	0.5	0.9	-0.7	0.4	0.1	419
209	-0.3	-1.7	-0.8	-1.2	-1.2	-1.2	-1.2	-0.5	-1.3		-1.1	0.2	398
CD		**-3.3**	**-1.9**	**-3**	**-1.8**		**-3.5**	**-2.1**			**-2.6**	**0.4**	**87**
AD		**-1.2**	**-0.8**	**-1**	**-1.3**		**-1.4**	**-1.3**			**-1.1**	**0.1**	**87**

Table 4: Mean daily percentage relative differences to RBCC-E reference at Huelva 2011 campaign for every instrument (lines) and day (columns), the three last columns show the average, standard error and number of simultaneous measurements for the overall period.(Reference Brewer and Dobson (CD and AD pair) are highlighted in bold)

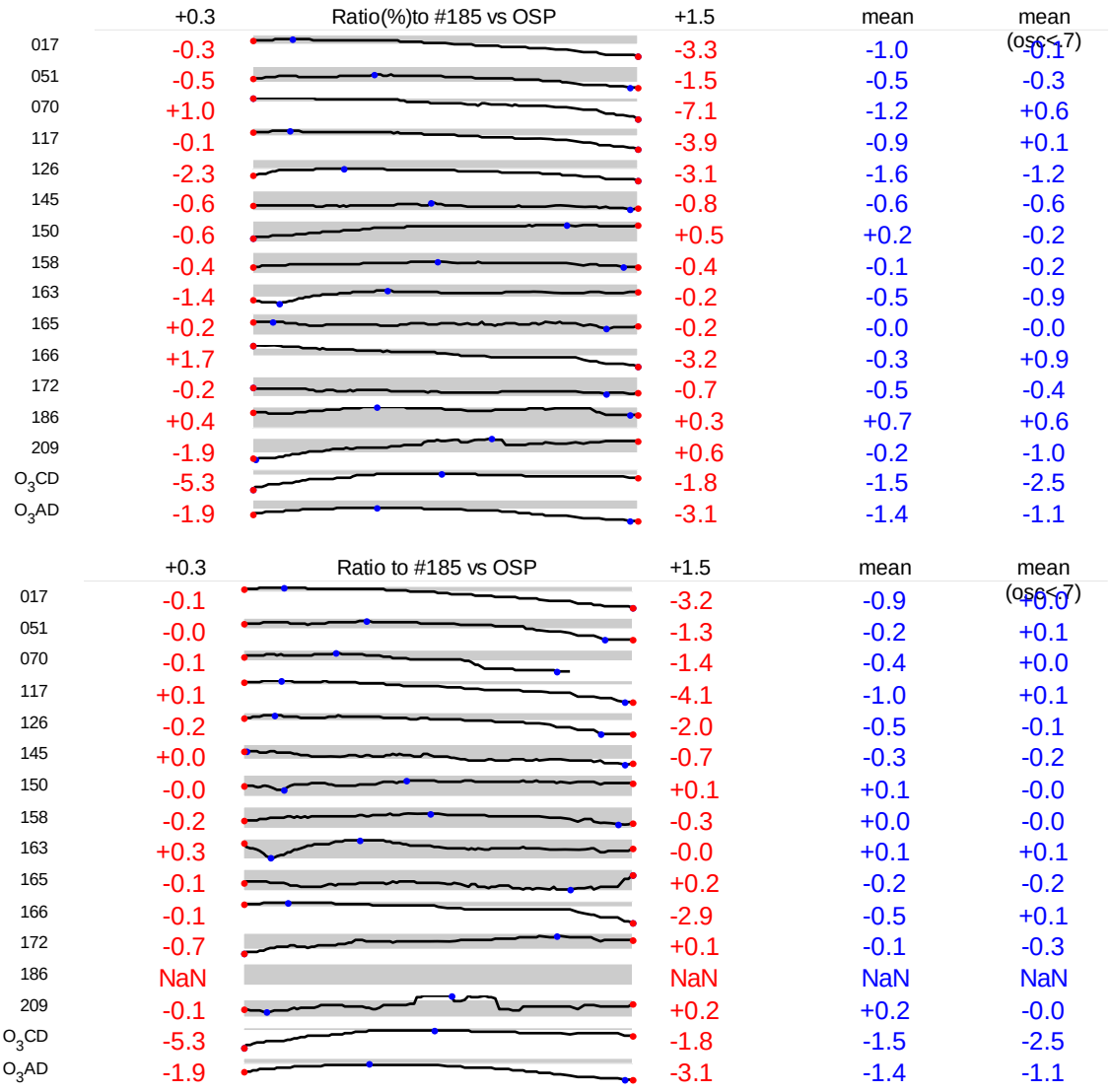

Figure 18: The table shows Sparkline percentage ratio of every instrument to RBCC-E reference against Ozone Slant Path (OSP) in the blind-comparison (upper panel) and with the final calibration (lower panel), in red the values at 0.3 and 1.5 OSP and in blue the mean value for the full range (0,3 1.5 cm) and for the observation with OSP<0.7 cm The grey area of the plot represents the +/- 1% on the upper panel and +/- 0.5 % on the lower panel

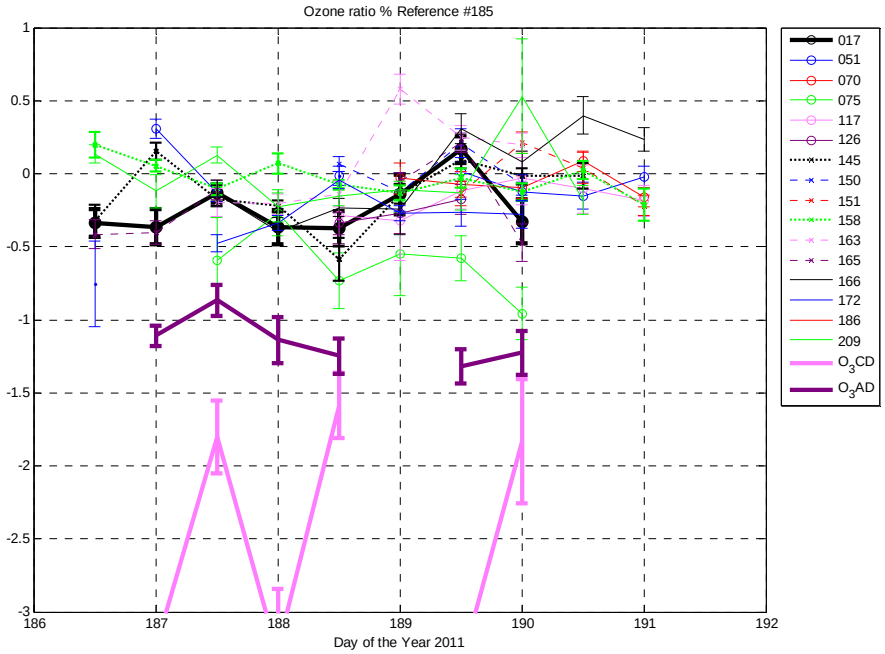

Figure 19: Final configuration daily ratios to the reference, all the brewer fall on the +/- 0.5% range

3.1.2.3 Nordic and Izaña campaigns

The Arctic contribution of CEOS intercalibration of Brewers and Dobsons took place at Sodankylä during the period March 8 to 23, 2011. Participation consisted of two Dobson and five Brewers teams. Unfortunately, the DMI instrument (Brewer #053), operated by Paul Eriksen was not operative for the complete intercomparison period, due transport problems. A complementary camping took place at Izaña during 28 of October to 17 of November with the participation of the FMI brewer #037 and brewer#107.

Institution	Name	Brewer/Dobson	Country
SMHI/SLU	Weine Josefsson Mikael Ottonsson	Dobson #064, Brewer #006-MKII	Sweden
DMI	Paul Eriksen	Brewer #053-MKII	Denmark
DWD RDCC-E	Ulf Köhler Herbert Munier	Dobson #30	Germany
FMI Sodankylä	Esko Kyrö Rigel Kivi	Brewer #037-MKII	Finland
FMI Sodankylä	Tapani Koskela Kimmo Rikkonen	Brewer #107-MKIII	Finland
AEMET RBCC-E	Alberto Redondas Juanjo Rodriguez	Brewer #185-MKIII	Spain

Table 5: Participants and Instruments at Nordic Campaign 2001.

The instruments were compared with the RBCC-E travelling reference Brewer#185. During the effective intercomparison period, nearly 400 simultaneous direct ozone measurements were collected, from a minimum ozone value around 310 DU to maximum ozone value around 450 DU. Artic solar conditions resulted in ozone slant paths spanning from 800 to 2000 DU. At Izaña the ozone range was of 30 DU from 260 to 290 and the OSP from 350 to 1600 DU. The objective of this exercise is to compare the calibration at these different locations with very different ozone and solar zenith angle. Could the calibration at Sondankyla (Figure 23) be still valid at Izaña six month later?

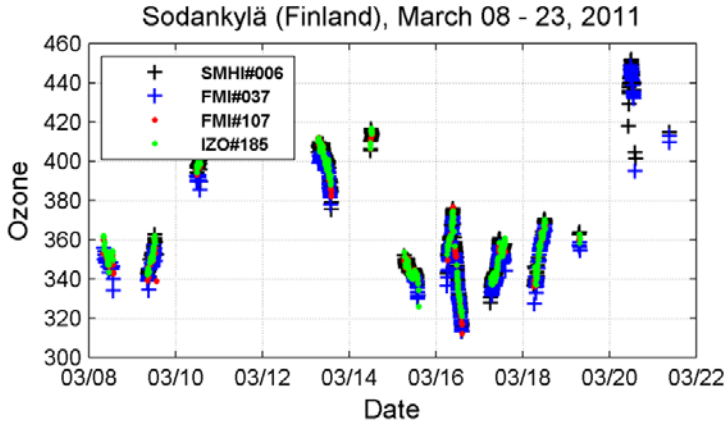

Figure 20: Ozone Direct Sun Measurements during the Sodankylä 2011 intercomparison

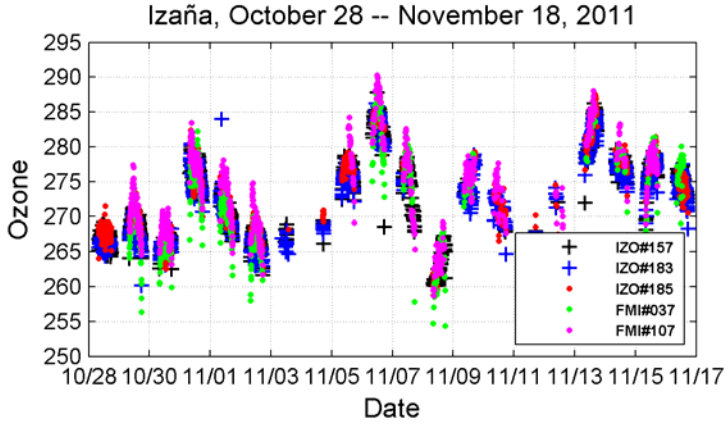

Figure 21: Ozone Direct Sun Measurements during the Izaña 2011 intercomparison

He-Cd laser measurements were used to characterize the slit functions of the single brewers. This data will be used to characterize the stray light effect on ozone measurements.

The main findings in this combined campaign are:

1) All the brewers at Sodankyla, double and singles, show an underestimation of 1% in the comparison with the RBCC-E reference (Figure 20). Notice that all these brewers are routinely calibrated by IOS.
2) This difference is not due to change or miss calibration of the reference (see section 3.1.2.1)

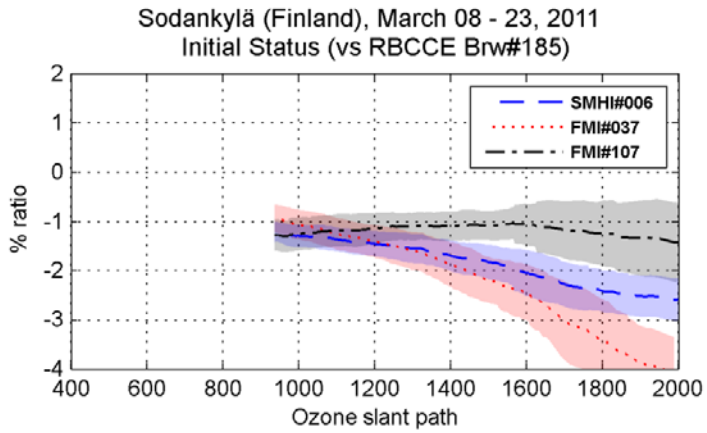

Figure 22: Percentage relative differences to the reference Brewer #185 vs. Ozone Slant Column of the instruments participating at Sodankylä 2011 campaign. Initial status. The straylight effect of single brewers (#006 and #037) is evident at high OSPs, at low OSPs all the brewers shows an underestimation of 1%.

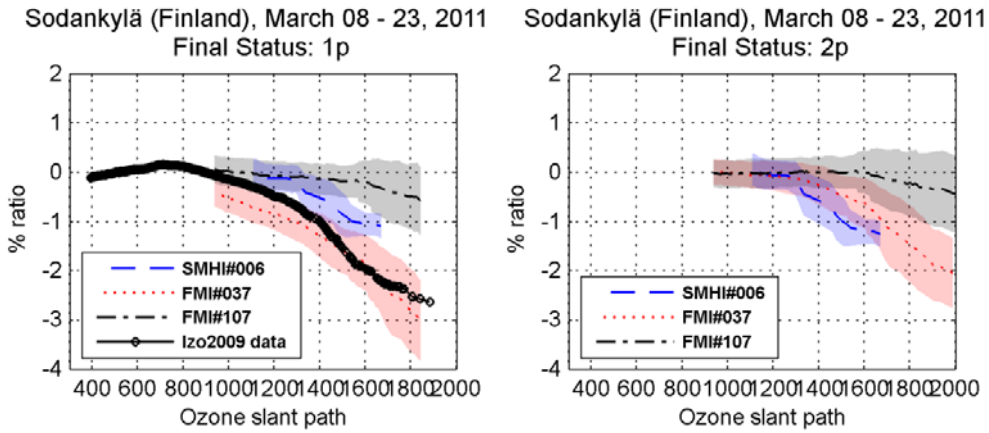

Figure 23: One parameter (right) and two parameter (left) calibration at Sodankyla

3) Brewer #006 show less stray light effect than #037, which are agree with the laser measurements performed at the campaign (Figure 21), modeling results are in progress.

4) The Brewer #037 has been compared three times with the RBCC-E instruments, IZO November 2009, Sodankyla March 2011, and IZO November 2011. The results of these comparisons are summarized in Figure 25. During the 2009 campaign, one could detect an issue with filter #3 which produced an irregular behavior near 450 DU (blue line). The instrument had been calibrated in 2008 by IOS and new calibration parameters were provided (red line). Basically the ozone absorption was adjusted to the measured value. The final calibration of Sodankyla are represented by the (thick pink line)

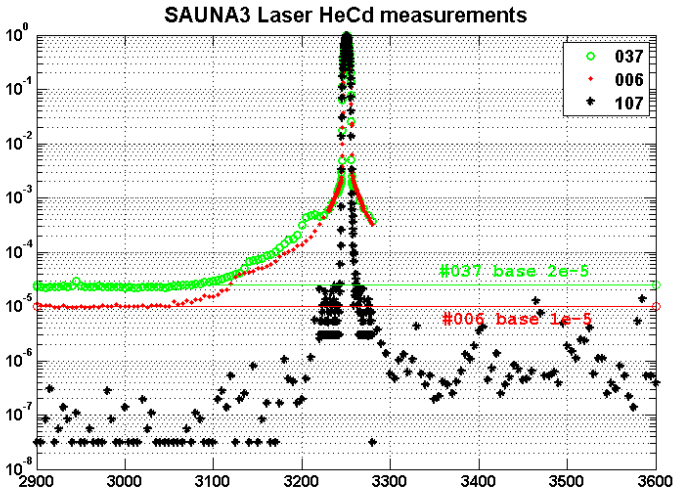

Figure 24: HeCd Laser measurements performed at Sodankyla, the stray light rejection is better in #006 compared to #037.

The comparison at Izaña 2011 shows that the IOS configuration is 0.5% lower (blue line), the 2009 RBCC-E calibration is valid if we apply the SL correction (black line) and the calibration performed at Sondankyla is valid at Izaña.
The calibration at high OSC for a bewer is quite difficult due the lack of sensivity of the ozone to changes in ETC. This was compensated for the big amount of observations and the apriori knowledge of the level of straylight of the instrument. The ETC determination only uses the observations taken at OSP lower than 1000.

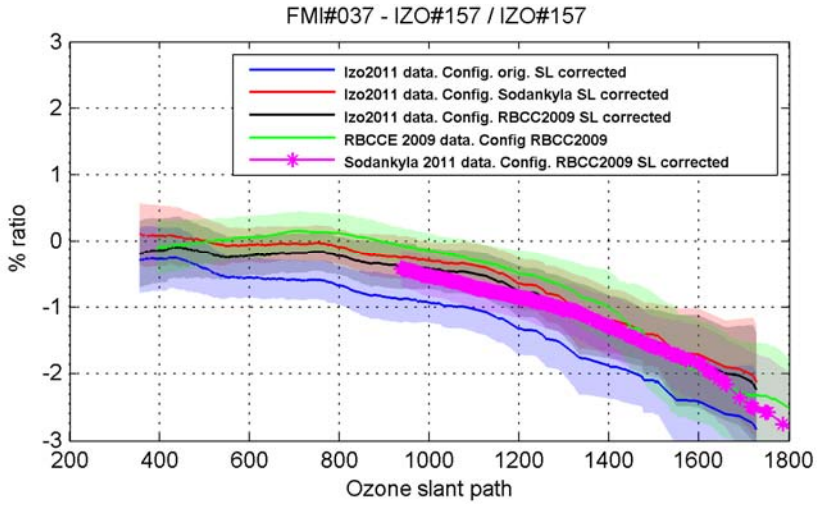

Figure 25: Relative differences of Brewer #037 to RBCC-E reference instrument #157 for direct sun ozone observations as a function of Ozone Slant Path. At Izaña 2009 using the RBCC-E calibration (green line), at Sondankyla 2011 using the same calibration (pink line) and at Izaña 2011 using three different calibrations: 1) IOS calibration July 2008 (blue line). 2) Sodankyla 2011 (red line) 3) RBCC-E Izaña Calibration 2009(black line).

5) For the brewer #107 we do not get so clear picture like the brewer #037. This is represented in Figure 26.

The instrument was calibrated and maintained during July 2010 by IOS. In this calibration, the instrument changed its constants due to photomultiplier adjustments. Like the other brewer at Sodankyla, its initial calibration was 1% lower, but in contrast with single brewer flat vs. OSC (black line). At Sodankyla a new calibration was provided (green line). During the comparison at Izaña the IOS calibration gives an underestimation of .5 % at OSC >1200 DU to 1.5 at 400DU. The calibration provided at Sodankyla seems to overestimate the ETC by 10 units and produces a 1% difference at 400 DU. This instrument presents a limitation due an anomalous SL ratio related with the temperature. The temperature dependence is not linear like for the other instruments and it is different for low temperatures and high temperatures. This issue with the temperature does not allow tracking properly calibration changes with the internal SL test.

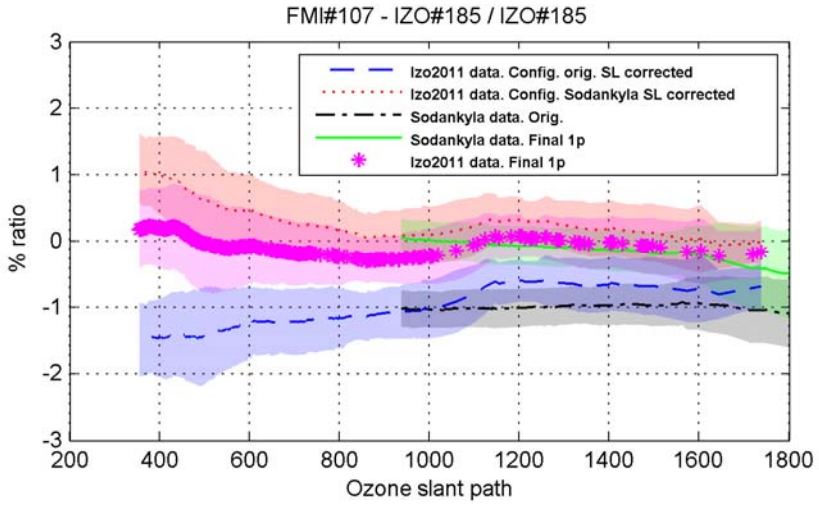

Figure 26: Total ozone per cent ratio to RBCC-E reference at Izaña using a) 2010 IOS (blue line). b) RBCC-E Sodankyla 2011 (red line) and c) Izaña 2011 RBCC final calibration respectively. Total ozone ratios at Sodankyla 2011 using a) IOS (black line) and b) RBCC final calibration (green line)

3.1.2.4 Brewer Dobson comparison

Brewer Dobson comparison at Huelva

Here we present the comparison of reference brewers (see below) and the Dobson #064 managed by RDCC-E. The brewers use their initial calibration (blind days) corrected by Standard Lamp (Table 4). The ratios use more than 300 simultaneous measurements (5 min) in the brewer case and around 90 in the case of the Dobson on the 0.3 to 1.5 OSC range.

The reference brewers enumerated below are routinely used to transfer calibration and have not been maintained at the campaign. With the exception of #017 from IOS all of them are double brewers.

1. #017: International Ozone Services travelling reference
2. #145: Environmental Canada double travelling reference
3. #158: Kepp & Zonen travelling reference
4. #185: RBCC-E travelling reference

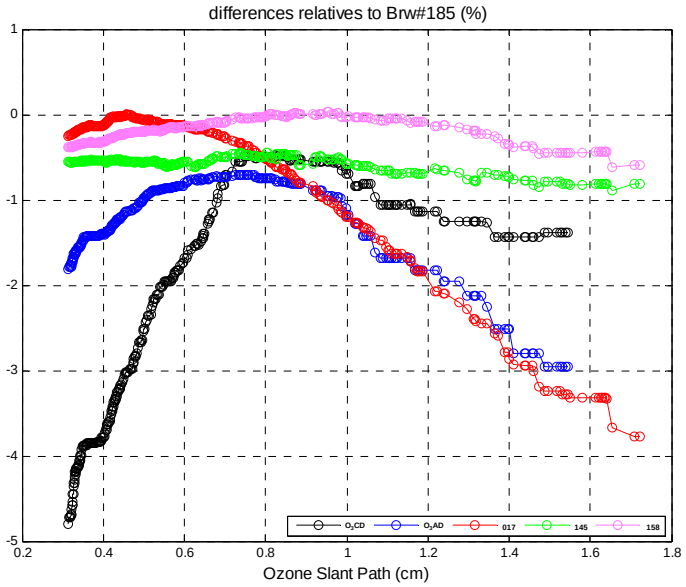

Figure 27: Mean Ratio to RBCC-E reference against ozone slant path (OSP), the mean is averaged form the simultaneous measurements at the campaign averaging observations with the same OSP +/- 12% of the OSP value

The comparison with the reference brewers is quite good (Table 4, Figure 17), the ratio against the RBCC-E reference #185 of the brewer #145 is -0.6% and even better for #158 (-0.2%). Finally the brewer #017 shows a mean difference of 0.4%.

The ratios for the Dobson 64 show a mean underestimation, against #185, of AD and CD pair observations of 1.1 % and 2.6% respectively. If we see the comparison on more detail, looking to the ratios against OSP (Figure 27), we notice that the Brewer #017 agreement is very good at low OSP, and underestimates the ozone due the straylight above 0.6 cm of OSP. In contrast the Dobson AD CD wavelengths ratios are lower (around 0.5%) at high OSP (0.8) and increase at lower and higher OSP near to -2% (AD) and -5% (CD) at 0.3 OSP and to -3%(AD) and -1.2% (CD). This suggests an ETC mismatch between Dobson 64 and RBCC-E reference. This is confirmed if we calibrate the Brewer#185 against the AD observations (Figure 28). The ozone absorption coefficient (slope) obtained is very close to the value used on #185 but the ETC if we use the Dobson as a reference is 1590, which is different from the reference ETC value by fifteen. Fifteen units in ETC are a considerable difference that we do not expect. As a test, we performed a Langley plot using the day 187 (6 of July) of the campaign when the recorded ozone was very stable, and we got an EC of 1580 very close to 1575 used during the campaign.

As we can see in section 3.1.2.1, the Langley plots before the campaign indicate an ETC of 1575 and we cannot detect any significant change on the #185 before and after the campaign in the comparison with the rest of RBCC-E triad.

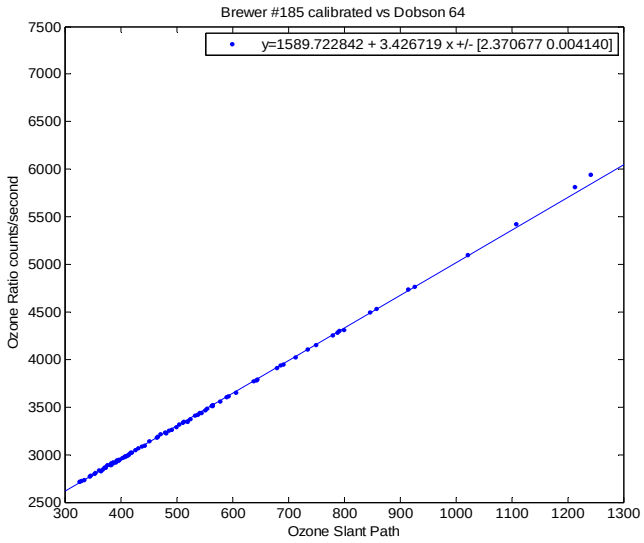

Figure 28: Brewer #185 calibrated using the Dobson 64 AD pair as reference

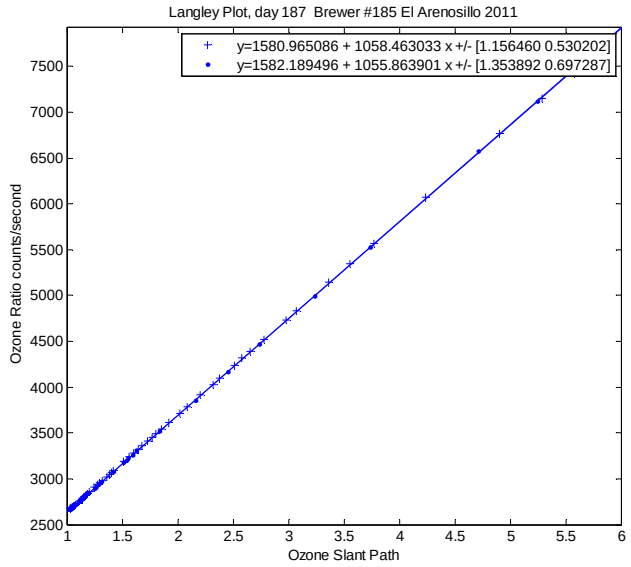

Figure 29: Langley Plot for the day 6 of July at El Arenosillo (morning and afternoon measurements cross and dots respectively).

3.1.2.5 Calibration instrumental issues detected during calibration campaigns

A big campaign like Arenosillo has the advantage to see the general view of the instrument calibration status and the disadvantage of the lack of time to see the instrument in closer detail. The 2009 and 2011 Arenosillo campaigns reveal some common instrumental issues who are not properly handled with the available tools.

The Huelva campaign reveals three important instrumental issues who affecting more than two thirds of the participating instruments. These three issues are:

1) Ozone absorption coefficient
2) Attenuation Filter
3) Dead Time setting
4) Stray Light

3.1.2.5.1 Ozone absorption coefficient

As we emphasized in the first progress report the ozone absorption coefficient (O3ABS) can be calculated from the dispersion test (one parameter calibration) or transferred from a reference instrument (two parameters calibration). Both methods will give the same results within the precision of the brewer instrument otherwise the wrong O3ABS setting produces a slope on the relative differences as function of OSP. The recommended method of calibration is the one parameter calibration; this means that the operative ozone absorption coefficient setting of the instrument must be very similar to the calculated one. This is not true for a significant number of instruments as shown in Figure 30. For more than two thirds of the instruments the discrepancies between the calculated o3abs and the setting is more than twice of the instrument precision.

3.1.2.5.2 Attenuation Filter

The brewer spectrophotometer uses neutral density filters in order to adapt the intensity of the light intensity reaching the photomultiplier. The light is maintained within certain level to maximize the signal to noise ratio. The ozone is calculated using ratios so if the filters are neutral they do not affect to the ozone calculation. In addition the weighing coefficients also verify:

$$\sum_{i=1}^{4} w_i \lambda_i = 0$$

Where "w" are the ozone weighing coefficients for wavelength λ

So a linear attenuation with wavelength does not affect the ozone calculation.

In a real instrument, some of the filters are not neutral; additionally the ozone wavelengths vary from instrument to instrument, and the second condition is only an approximation. As a result of this nonlinearity the calculated ozone depends of filter used in the measurement. This is clear when the instrument is compared with a reference and the differences are grouped by filters. Up to 20 ETC units (around 2% in ozone) has been observed during the campaign (Table 6).

If we know the attenuation of the filter j for the ozone wavelength (λ) A_{jl} can be easily corrected introducing an ETC correction for every filter.

$$FC(j) = \sum_{\lambda=1}^{4} w_\lambda A_{j\lambda}$$

Several methods have been developed to determine the wavelength dependence of the filter, using the internal lamp (FI routine), using the sun as source (AT routine) or using the Langley extrapolation. This non linearity is difficult to determine with precision and frequently the results are not significant with the number of tests that can be performed during a campaign. Furthermore the Filter Correction (FC) can be determined directly by examining the historic record of the instrument and looking for the simultaneous measurements performed with consecutive filters or filtered by comparison to a reference instrument (see Brewer Workshop presentation for details).

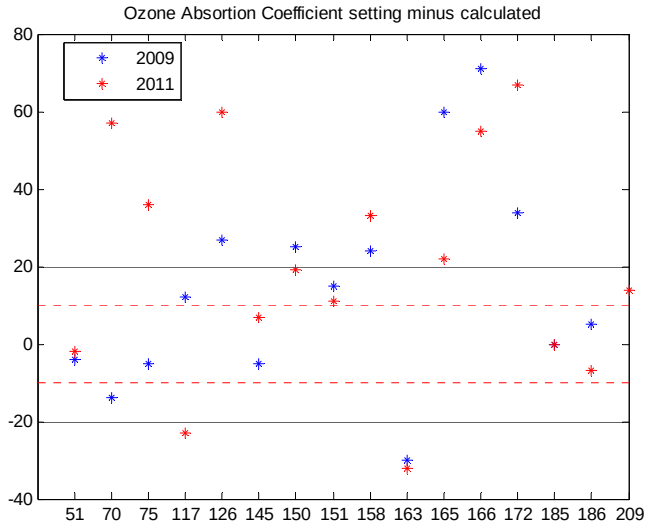

Figure 30. Difference between the ozone absorption setting and the calculated in 2009 (blue) and 2011 (red) campaign. The blue line represents the estimated wavelength resolution of the brewer (1 micrometer step) and the red line the double (2 micrometer steps), that can be translated to ozone calculation of 0.3% and0.6% respectively.

At Arenosillo 2011 more than two thirds of the instruments show a filter issue. The effect in ozone is only important at low air masses which implies high attenuation filter (>=F#4). This high filters are seldom used in mid-latitudes stations and may not affect to the ozone series.

	17	51	70	75	117	126	145	150	151	158	163	165	166	172	185	186	209
F#1		0	0	0	0	0	0	0	0	-3	0	0	0	0	0	0	0
F#2	0	0	0	0	0	0	0	0	0	-6	0	0	0	0	0	0	0
F#3	0	0	0	0	0	N/A	0	0	0	-9	0	0	7	-10	7	0	0
F#4	0	0	0	10	0	0	0	-15	0	0	0	-18	0	-10	15	0	0

Table 6: Filter correction determined at Huelva 2011,

3.1.2.5.3 Dead Time

The Brewer photomultiplier measures the radiation in photon counting mode, in this mode not every photon incident on the primary surface is counted because a second photon can arrive at the photomultiplier during the "dead time" associated with a first photon and never be noticed. One estimate the dead time by measuring two wavelengths using the internal lamp, these wavelengths can be measured independently or simultaneously. Applying the Poison statistics to estimate the counts missed by the counting system, the DT constant is calculated imposing the condition of the counts measured with first wavelength plus the second equals the counts when measuring the two wavelengths simultaneously (See brewer SOP for details). The Brewer SOP recommends that the DT constant will be inside two nanoseconds (ns) of the measured value.

The effect of a discrepancy in the DT on the ozone is not simple and depends of the recorded intensity, which in turn depends of the attenuation filter used, and the spectral response of the brewer. This dependence on the spectral response makes the DT be bigger on a single brewer monochromator, up two 2% for a 4 ns difference, than in double brewer 0.4 % for the same difference (Figure 31).

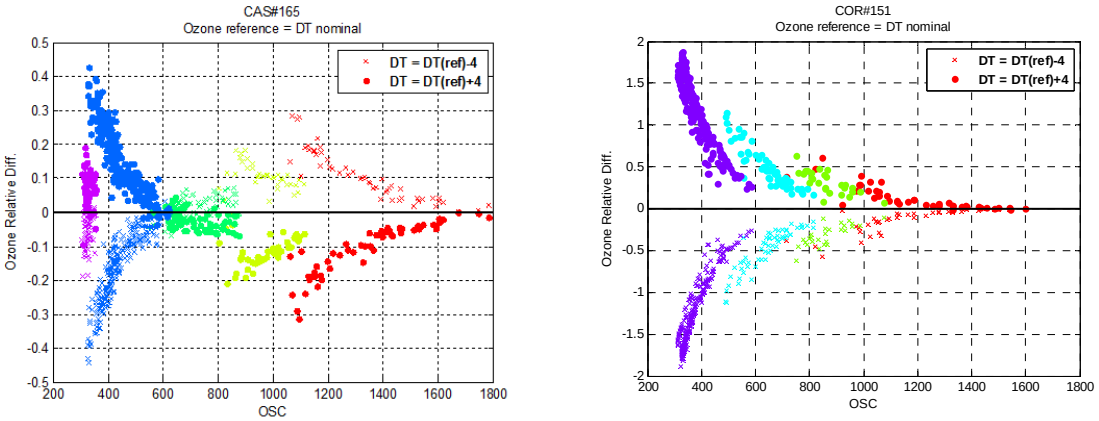

Figure 31. Ozone relative differences for a mismatch of 4ns (cross +4ns , dots -4ns) for a double (left) and double (right). The different colours represent the attenuation filter used on the measure.

Looking at the participating brewers during the Arenosillo campaign (Figure 32), we found that around two thirds of the brewers measure a DT constant more than 4 ns, different of the setting. (4 ns is the double of the recommended tolerance). We also see in this figure that in some brewer's low intensity and high intensity measures differ and the calculation could be affected by the lamp brightness, this behaviour is not fully explained and a new method of measurement of the DT constant is on developing using the sun as a source.

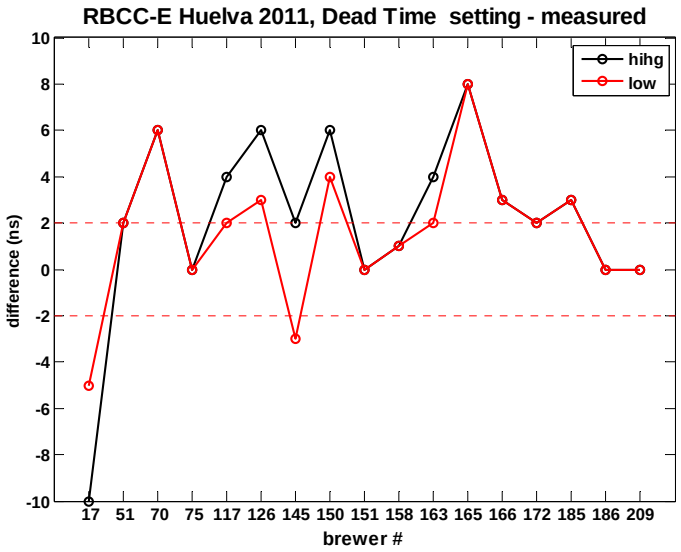

Figure 32. Dead Time setting minus measured at Huelva campaign for all participating instruments. The DT time is performed with different attenuation filter, low intensity test (high attenuation filter) are in red and high intensity are in black.

3.1.2.5.4 Stray Light

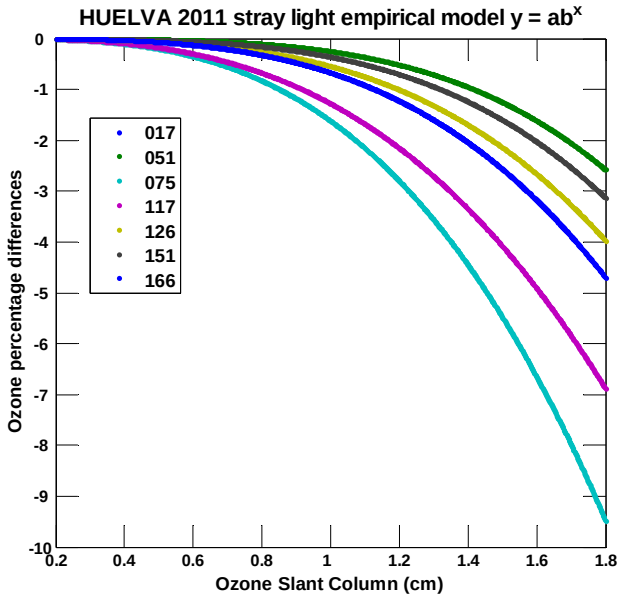

Figure 33. Empirical model fit of the ozone percentage differences against the RBCC-E reference for the single monochromator brewers at Huelva 2011 campaign.

The underestimation of ozone of single monocromators brewer due the stray light was already discussed on the previous report. Here we show the statistical results of the single brewer at Huelva

campaign; the relative differences of the single brewers against the RBCC-E reference are fitted to a power function are shown on Figure 33. Based on previous studies (Mc Linden et all, 2007) we expect that the brewers will be grouped according to the stray light characteristics (Brewer type I,II of the McLiden work). However preliminary results at Huelva show that this grouping is not evident. The analysis of the stray light characteristic of this particular brewer, and the stray light modelling are now an ongoing activity of the project.

3.1.2.5.5 Summary

One of the important findings on this campaign is when we put all this information together (Table 7) the instruments affected by Filter issues are the same instruments than the O3Abs coefficient in use are not agree with the dispersion measurements. A mismatch of the O3Abs produces a slope on the relative differences as function of slant path; this slope can compensate the filter effect. It is not unreasonable to think that in the absence of software tools to correct the effect of the filter on the ozone calculation, this effect is compensated with the adoption of an unreal absorption coefficient.

	17	51	70	75	117	126	145	150	151	158	163	165	166	172	185	186	209	Total
O3ABS				X		X		X		X		X	X	X				40%
Filter				X		X		X		X		X	X	X	X(*)			47%
DT	X		X			X		X			X	X						35%

Table 7. Summary of the instrument affected for Ozone absorption, Filter issues and Dead Time. (*) Brewer #185 ozone results are filter corrected.

3.2 Exploitation of results from the 2009 CINDI campaign

3.2.1 Intercomparison of MAXDOAS formaldehyde slant column measurements

Although the capabilities of MAXDOAS systems for HCHO detection has been demonstrated in several past studies (e.g. Heckel et al., 2005; Wagner et al., 2011), no effort has been devoted yet to harmonize instruments and retrieval methods. Such activities are an essential prerequisite for the reliable retrieval of vertical columns and profiles from MAXDOAS HCHO measurements. Therefore we have taken the opportunity of the Cabauw Intercomparison Campaign of Nitrogen Dioxide measuring Instruments (CINDI) campaign where a number of MAXDOAS instruments have been jointly operated (Roscoe et al., 2010; Piters et al., 2012) to asses for the first time the consistency of these HCHO measuring systems (for more details on the present study, see Pinardi et al., 2012). The Cabauw site is located in a semi-rural area of the Netherlands where formaldehyde concentrations are expected to be comprised between one and several tens of ppbv, which are typical levels of the background continental boundary layer and urban regions, respectively (Fried et al., 2011; Hak et al, 2005). In their study on multi-component MAXDOAS retrievals during CINDI, Irie et al. (2011) reported median HCHO vertical mixing ratios (VMR) of around 2.5 ppbv, and peak values of up to 8 ppbv.

A detailed description of the CINDI MAXDOAS instruments can be found in Piters et al. (2012) and Roscoe et al. (2010), and additional references relevant for the present study are given in Table 8. All systems operated during CINDI were set up to record spectra at a set of prescribed elevation angles (3°, 4°, 8°, 15°, 30° and the zenith), and at the fixed azimuth angle of 287° relative to North. A full cycle of MAXDOAS measurements was generally obtained within half an hour. For the intercomparison of HCHO, only measurements recorded at solar zenith angle (SZA) less than 75° were used in order to exclude error-prone twilight measurements, not relevant for the present study.

Table 8. Main characteristics of the spectrometersinvolved in the HCHO intercomparison campaign.

Institute	Measurement Period for HCHO	FWHM (nm)	Detector characteristics	Integration Time	Reference
BIRA	13/6 to 22/7	0.38	back-illuminated CCD, 2048×512 pixels (-30°C)	60s	Clémer et al., 2010
INTA	7/7 to 24/7	0.4	UV enhanced CCD, 1024 pixels (-30°C)	50s	Roscoe et al., 2010.
Bremen	8/6 to 21/7	0.4	back-illuminated CCD, 2048×256 pixels (-35°C)	40s	Wittrock et al., 2004
Heidelberg	17/6 to 2/7	0.5	back-illuminated CCD, 2048×256 pixels (-30°C)	60s	
JAMSTEC	8/6 to 24/7	0.7	uncooled CCD, 3648 pixels	5 min	Irie et al., 2011
NASA	22/6 to 20/7	0.6	uncooled CMOS	20s	Herman et al., 2009
WSU	21/6 to 5/7	0.83	back-illuminated CCD, 2048×512 pixels (-70°C)	Typical 1.2s	Herman et al., 2009
Toronto	30/6 to 4/7	0.2 – 0.8	back-illuminated CCD, 2048×512 pixels (-72°C)	30s	Fraser et al., 2009

Mainz	21/6 to 10/7	0.6	Stabilised CCD, 2048 pixels (4°C)	60 s	Shaiganfar et al., 2011

For this intercomparison exercise, standardized analysis settings were defined and prescribed, based on experience and heritage from past studies. These settings are summarized in Table 9. Note that absorption cross-sections were all convoluted at the resolution of the individual instruments using slit function information provided by each group. In the case of O3 and NO2 cross-sections a solar I0 correction has been applied (Wagner, 1999; Aliwell et al., 2002).

Table 9. Baseline DOAS analysis settings used for HCHO slant column retrieval during the intercomparison exercise.

Parameter	Specification
Fitting interval	336.5-359 nm
Wavelength calibration	Calibration based on reference solar atlas (Chance and Kurucz, 2010)
Cross sections	
HCHO	Meller and Moortgat (2000), 293°K
O_3	Bogumil et al. (2003), 223° and 243°K, I_0-corrected
NO_2	Vandaele et al. (1996), 220°K, I_0-corrected
BrO	Fleischmann et al. (2004), 223°K
O_4	Hermans et al. (2003) (http://spectrolab.aeronomie.be/o2.htm)
Ring effect	Chance and Spurr (1997)
Closure term	Polynomial of order 3
Intensity offset	Linear correction
Wavelength adjustment	All spectra shifted and stretched against reference spectrum

For the retrievals, daily reference spectra were taken from the zenith elevation around 11h40 UT. Figure 34 presents an example of HCHO fitting result obtained with the BIRA-IASB instrument on 30th June 2009, at 4° elevation angle and 43° SZA. The corresponding residuals (approximately 10-4 RMS) are typical of low-noise scientific grade instruments. Under similar conditions, residuals can be an order of magnitude larger when using compact mini-DOAS systems.

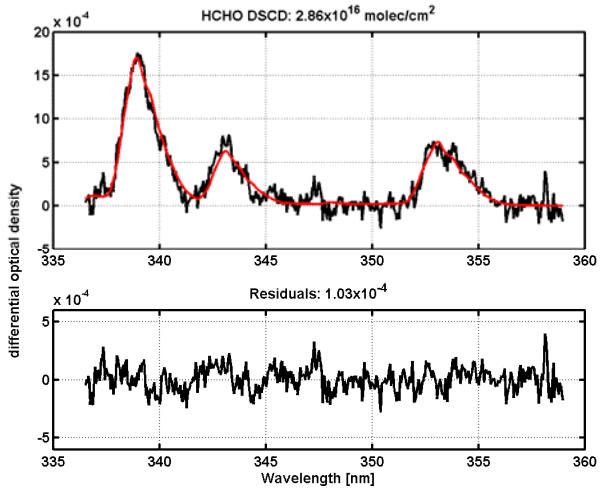

Figure 34. Example of a HCHO slant column fit obtained with the BIRA-IASB instrument on 30 June 2009, around 14h30 (UT time), at 4° elevation angle and 43° solar zenith angle.

To intercompare the various DSCD measurements, we have followed the method introduced in Roscoe et al. (2010) for the NO_2 and O_4 slant column measurements intercomparisons, also already described in our previous progress report. HCHO DSCDs retrieved by each group were averaged over periods of 30 minutes. This procedure minimizes the impact of the temporal and spatial variability of HCHO and of the differences in read-out noise between instruments. An example of the diurnal evolution of the resampled HCHO DSCDs is shown in Figure 35 for different elevation angles, on 2nd of July 2009. This day was chosen because almost all instruments were in operation and the HCHO concentrations had a smooth variation over time. As can be seen, the HCHO DSCDs are consistently larger at low elevation due to enhanced light path in the near-surface HCHO layer; also the different groups agree reasonably well with each other.

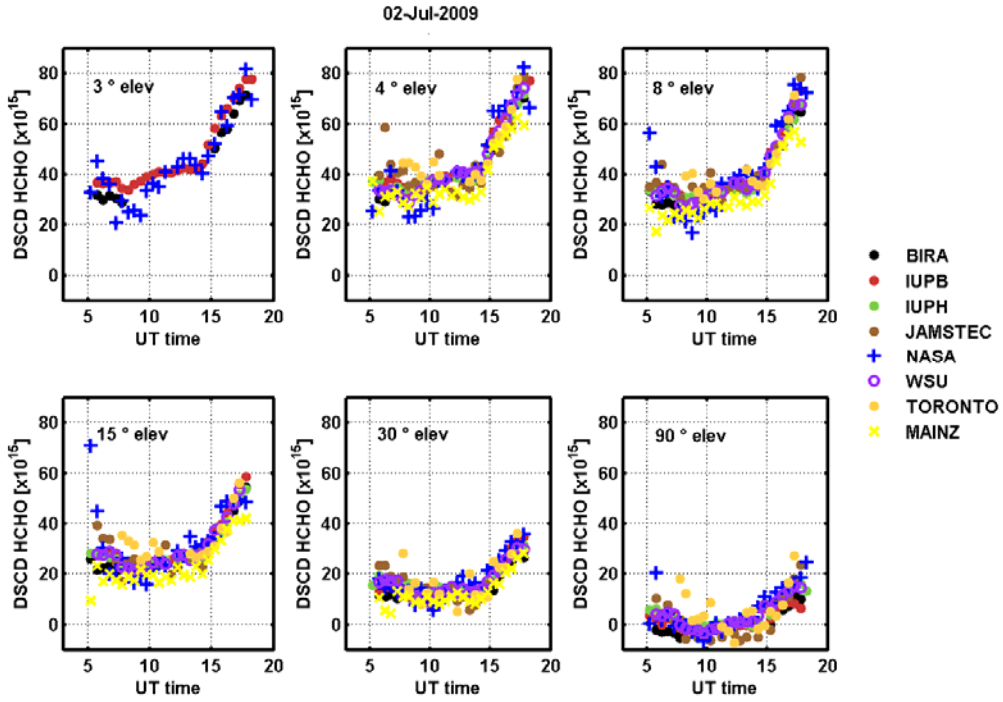

Figure 35. Diurnal evolution the HCHO DSCD measured on 2 July 2009 and averaged in bins of 30-minutes duration, for the different instruments involved in the intercomparison. Units are molec./cm². It should be noted that on this day, not all groups have been measuring at all elevations (e.g. only a few groups reported data at 3° elevation).

To proceed further, a reference data set was created by grouping the instruments that presented the best mutual agreement. Accordingly a reference data set was created by averaging data from the Bremen, BIRA and INTA instruments. The scatter plots displayed in Figure 36 illustrate, for the 4° elevation case, the results of the final comparison where data from each individual instrument are compared to the merged reference. Although the number of coincident points can differ a lot depending on instruments, most of the groups are found to agree quite well with the reference. Figure 37 presents the final results of the statistical analysis, constructed using the whole ensemble of off-

axis measurements (3°, 4°, 8°, 15° and 30°). Most instruments compare relatively well with the reference for most of the elevation angles: correlation coefficient are close to unity (illustrating the compactness of the scatter plot with respect to the reference), slopes deviate by no more than 15% from the reference and intercepts are close to zero. Note that larger discrepancies are systematically obtained at 30° elevations due to the smaller HCHO DSCDs at this elevation angle. Also larger discrepancies are found for the JAMSTEC and NASA data sets, which might possibly be connected to the larger noise of the corresponding instruments with respect to others.

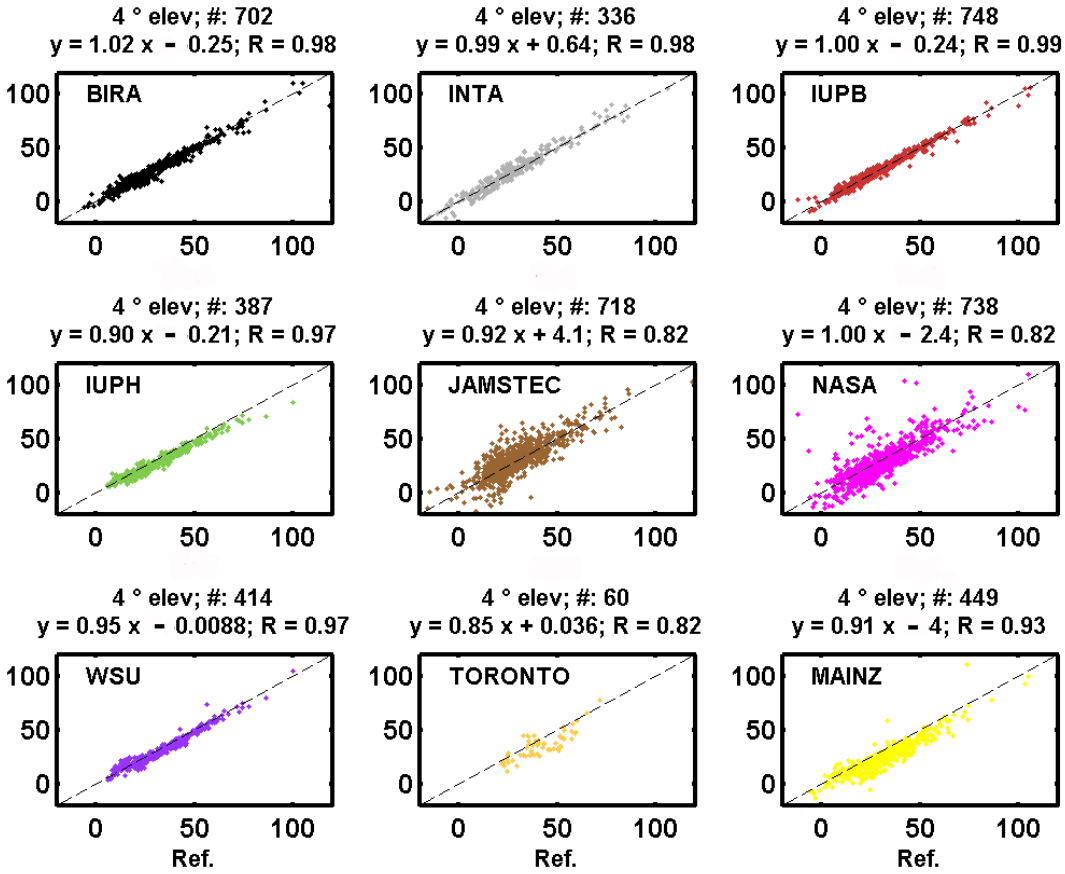

Figure 36. Scatter plots of HCHO DSCDs measured by each instrument compared to the campaign reference data set (see text), for the case of measurements at 4° elevation angle. Statistical parameters derived from the regressions (number of points, linear regression equation and correlation coefficients) are given on top of each subplot.

Owing to the harmonization procedure adopted in this work, the results presented here can be considered as representative of the level of consistency between HCHO measuring systems operated during CINDI. To better assess the error budget of the technique, additional tests were performed. The total uncertainties can be divided into two categories: (1) the random errors mostly caused by measurement noise and (2) errors affecting the slant columns in a systematic way. In order to evaluate the systematic contribution, we performed various sensitivity test using selected spectra from the BIRA instrument recorded on a clear day with a non-negligible amount of formaldehyde (4th of July 2009).

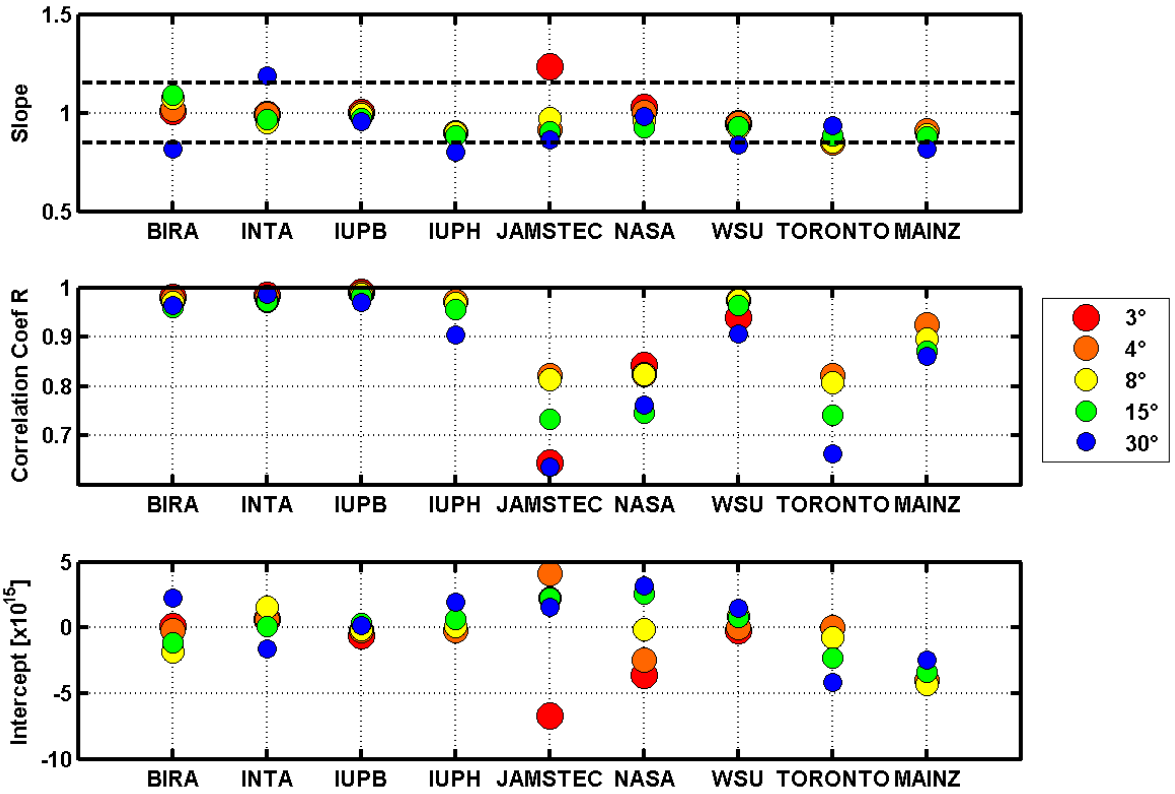

Figure 37. Straight-line slopes, correlation coefficient and intercept of HCHO slant columns against those of the reference, for each instrument and all off-axis elevation angles. The dotted lines in the first subplot correspond to values of 1.15 and 0.85.

Table 10 and Figure 38 summarize the results from the sensitivity study. For most cases considered, the retrieved HCHO slant columns fall within 15 to 20% of the values obtained with the baseline settings. The largest deviations are found to be related to uncertainties on the Ring effect cross-sections, as well as the O4 absorption cross-sections. The degree of the closure polynomial also appears to be an important source of uncertainty. These three effects contribute to 5-35%, 15-20% and 2-18% of the observed variability in the retrieved HCHO, respectively. Assuming that the different effects are sufficiently uncorrelated with each other, we can sum up all deviations in quadrature to obtain an estimate of overall systematic uncertainty which is represented by red squares in Figure 38. On this basis, we estimate that systematic uncertainties are around 20-40% with larger values at large SZA. Since some of the effects considered in our study are likely to be correlated, at least to some extent, these values could be considered as upper limits. However, and despite our efforts to include the most important sources of uncertainties in our sensitivity analysis, the need for possible additional terms cannot be excluded a-priori, so arguably the uncertainties reported here are to be interpreted as realistic conservative values.

Table 10. Results of sensitivity tests on HCHO slant column retrievals. See text for details about the different parameters changed.

Parameter changed	Relative HCHO difference [%]	Absolute HCHO difference [molec./cm^2]
Slit function fit	Within ±4%	± 2x10^{15}
Calibration	Within ±5%	± 3x10^{15}
Reference absorption cross-sections		
HCHO	9%	6x10^{15}
O_3	~8%	3x10^{15}
BrO	2%	-2 to 6x10^{14}
O_4	-10 to -30%	-8x10^{15}
Ring effect		
Case A	-40 to 55%	-10 to 12x10^{15}
Case B	-20 to 30%	-4 to 8x10^{15}
Case C	-20 to 40%	-4 to 9x10^{15}
Polynomial degree		
4th order	0 to -15%	-4 to -2x10^{15}
5th order	-5 to 40%	-5 to 15x10^{15}
Fitting window limits		
335-357nm	-10 to 15%	-4 to 6x10^{15}
335-356nm	-10 to 20%	-4 to 8x10^{15}
334.5-356nm	-15 to 40%	-5 to 12x10^{15}

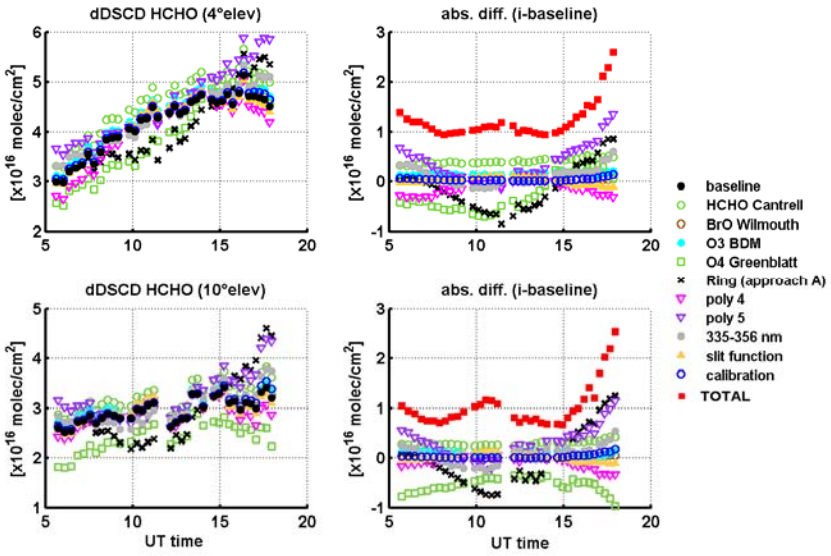

Figure 38. Summary results from the analysis performed to evaluate the sensitivity of the retrieved HCHO dDSCDs for various changes of the DOAS analysis settings, using data from 4th July 2009 and for the cases of measurements at 4° and 10° elevation angles. The total uncertainty on HCHO dDSCD (red squares) is estimated by adding in quadrature the different contributions.

Based on these results, an overall assessment of the total uncertainties on HCHO DSCDs has been generated. It is represented in Figure 39 for the 4° elevation case. Total absolute errors are found to be comprised between 1x1016 and 2-2.5 x1016 molec./cm², which approximately corresponds to relative errors ranging from 20 to 50 % for large to medium HCHO columns. Considering individual measurements from scientific grade instruments, one can see that total errors are largely dominated by the systematic part. An opposite behavior is found for mini-DOAS-type instruments where both random and systematic uncertainties contribute similarly. The random uncertainty can be reduced by means of longer integration times. Hence, for less sensitive mini-DOAS instruments, a trade-off between error and time resolution has to be made.

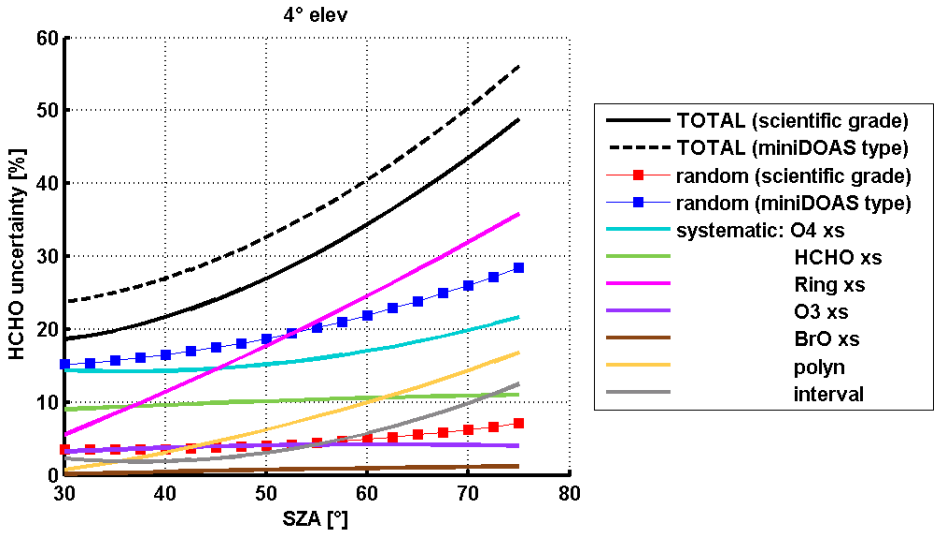

Figure 39. Summary assessment of the error budget on HCHO dDSCD, as a function of the SZA. Random uncertainties typical of low-noise scientific grade instruments and of mini-DOAS types of instruments are given separately.

3.2.2 Measurements of NO_2 profiles with MAX-DOAS: theoretical and practical case studies as part of the CINDI campaign

During the CINDI campaign, the slant column retrievals of NO_2 and O_4 from all participating instruments were evaluated in a semi-blind intercomparison (Roscoe et al., 2010), and agreement within 10% (5% for most instruments) was found for both species (see previous progress report). This illustrates the fact that in spite of their technical differences, the participating MAX-DOAS instruments yield consistent results for the NO_2 and the O_4 slant columns. The latter have been included in the intercomparison exercise since they are commonly used to determine the aerosol content in the atmosphere, which has a large impact on the weighting functions for the trace gas retrieval. This aspect is investigated in detail in Frieß et al. (manuscript in preparation) using results from CINDI and other campaigns.

Here, nine MAX-DOAS retrieval methods were compared by applying them to both modelled and measured data sets of NO_2 slant columns. The focus is on tropospheric columns and surface mixing ratios, the two most frequently used retrieval results. The first data sets used are modelled NO_2 slant

columns for a total of 16 different scenarios (eight NO_2 profiles and two aerosol scenarios) at realistic viewing conditions for a typical day during the CINDI campaign. This exercise has the advantage that all relevant input parameters are known and differences in results should be due to retrieval techniques only. The second comparison is on the retrieval of real data using fixed settings for all "Optimal Estimation"-like retrieval techniques. Only CINDI data from the Bremen instrument have been analysed to avoid differences in NO_2 results due to different instrument characteristics or observation parameters. In the last set of comparisons, all groups used their own data and their own "best settings" retrievals. The results are then compared to complementary measurements from in situ instruments, an NO_2-lidar, and NO_2 sondes, providing end-to-end validation of the different MAX-DOAS observations.

3.2.2.1 Profile retrieval algorithms

This section describes briefly, how the different groups retrieve trace gas profile information from their MAX-DOAS measurements. All retrievals shown here based on slant column densities (SCDs) described in Roscoe et al. (2011). Here also details on the settings used for the DOAS analysis of the spectra and therefore for the calculation of the SCDs are given.

In principle two different profile retrieval approaches have been used to analyse simulated and real MAX-DOAS data of NO_2 in this intercomparison. Six groups (IASB-BIRA, IUP Bremen, IUP Heidelberg, Universities of Leeds and Leicester, NIWA and Washington State University) apply full inversion methods by describing the relation between measurements (SCDs of trace gas for different elevations) to the absorber profile as a linear problem. This is solved by using a priori information and the Optimal Estimation method (Rodgers et al., 1990) and by doing online calculation of so called block air mass factors (BAMF). Three others (JAMSTEC, KNMI, MPI Mainz) prefer to use simpler parameterisation methods i.e. reducing the retrieved profile to two to three independent parameters usually by assuming a block profile for the trace gas and retrieving the layer height and the mixing ratio in this layer.

3.2.2.2 Results

The extensive NO_2 data set obtained during CINDI has enabled us to perform in-depth intercomparisons. These will point to the possible origins of differences in the derived geophysical parameters, and whether they are related to instrumental, algorithm, or interpretation differences.

3.2.2.3 Simulation study

Here one of the partners (BIRA-IASB) has calculated NO_2 slant columns both in the UV and in the visible for eight different NO_2 scenarios (profiles, see Figure 40) and two aerosol loadings (AOD 0.14 and 0.54 at 477 nm) using the radiative transfer model LIDORT. The simulation has been carried out applying boundary conditions (meteorology and viewing geometry) from June 24, 2009 in Cabauw. Slant columns for elevation angles similar to those chosen in the intercomparison exercise (Roscoe et al., 2011) have been provided and used as input for the profile retrievals (1°, 2°, 4°,5°, 6°, 8°, 10°, 15°, 30°, 89°). The SCD error included, based on real DOAS fit errors plus Gaussian noise. Since this exercise focusses on differences in the trace gas retrieval only, aerosol parameters like extinction profile, single scattering albedo and phase function were provided to the participants. All OE-type retrievals used similar settings for their calculations (e.g. a linear decreasing a priori profile). More technical aspects have been investigated by using e.g. different

altitude grids (50 and 200m) and different a priori errors. With the exception of MPI all other groups were able to calculate profiles both for the UV (360 nm) and the visible (477 nm).

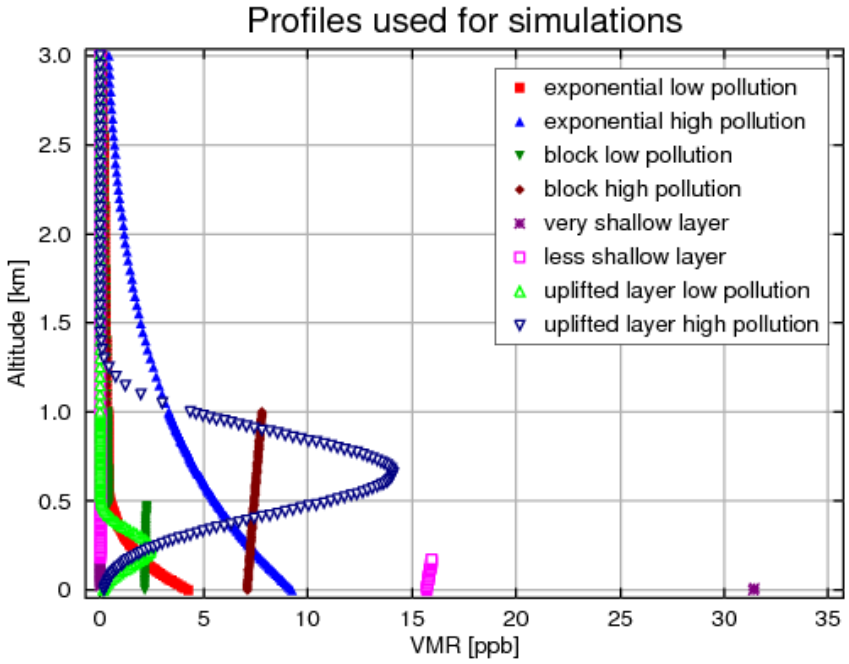

Figure 40. The profiles shown here have been used for the simulation of SCDs. The sequence for the profiles is the same as in the following figures.

In Figure 41 and Figure 42 some of the results of the simulation study are illustrated exemplarily. It has been shown that for the most important parameters – the NO_2 tropospheric vertical column and the NO_2 mixing ratio close to the surface – the different MAX-DOAS methods are able to reproduce the truth within 25% even for higher aerosol (AOD=0.54) and more difficult scenarios like uplifted NO_2-layers.

The retrieval in the visible (at 477 nm) is more stable and results are closer to reality than in the UV (at 360 nm) which is mainly due to the lower impact of aerosols. Even with a simple geometric approach it is possible to identify in average the right number for the tropospheric column. However, the standard deviation is much higher and the method fails for complex viewing geometries, e.g. small relative azimuth angle and solar zenith angles above 75°. The performance of the different retrieval methods is quite similar. With exception of JAMSTEC and to a lower extent KNMI all approaches are for most scenarios within the selected limits even for higher aerosol and difficult viewing geometries.

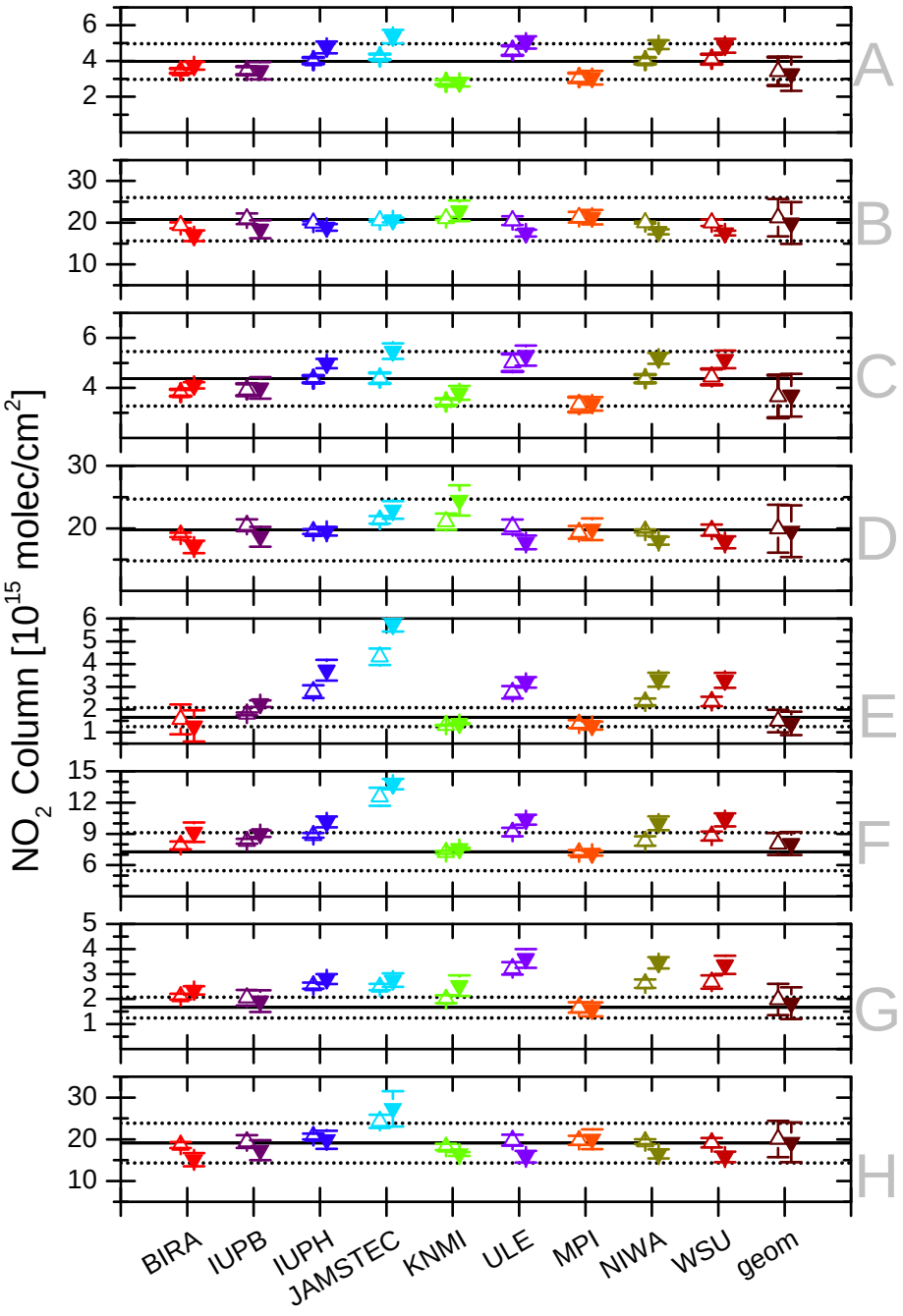

Figure 41. Retrieval results for tropospheric vertical columns. Shown are the daily means in the UV (360 nm) for the scenarios illustrated in Figure 40. Error bars indicate the standard deviation (28 profiles, one for each 30 minutes, are included). Open symbols reflect low aerosol, filled high aerosol. In addition to full retrievals, results using a simple geometric approach are shown. Lines indicate true values plus/minus 25%.

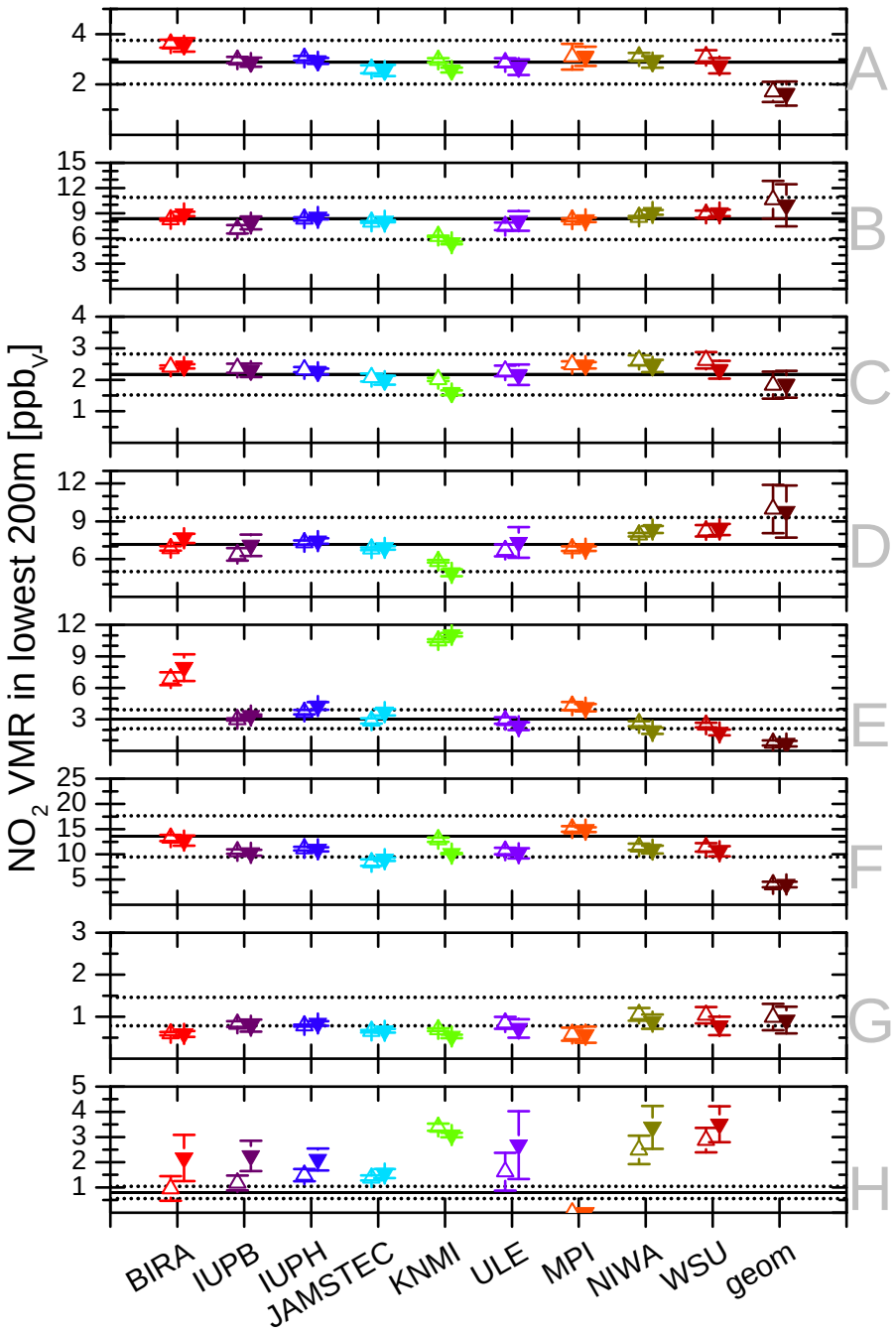

Figure 42. The same as Figure 41 but for the VMR in the lowest 200m. Here lines indicate true values plus/minus 30%.

3.3 EARLINET measurement campaigns

The intercomparison measurement campaign program is based on the idea of checking the performances of the lidar systems performing measurements with several lidar systems in the same site and in different meteo and light conditions. Indeed, this intercomparison program is part of a wider strategy addressed to intercompare the systems at all levels: not only at instrument level, but also at algorithm level.

This strategy includes several steps:

- development of instrumental standard tools for internal quality check of the performance of the instruments
- definition of standards (deviations, signal to noise ratio, maximum and minimum range) to accept a system in terms of performances suitable for EARLINET QA data
- development of a common data pre-processing and processing calculus system (Single Calculus Chain) suitable for all the lidar systems, able to fast pre-process and process data and to fast reduce the data at the same resolution
- definition of the mobile reference lidar systems within EARLINET
- on site intercomparison of the lidar reference systems
- on site intercomparison of all the EARLINET lidar systems with the lidar reference systems

Five intercomparison measurement campaigns were carried out in 2009 and 2010: EARLI09, ALI09, SOLI10, ROLI10 and SPALI10 as reported in the following table:

Campaign name	Location	Date
EARLI09 [11 lidar systems] (EArlinet Reference Lidar Intercomparison campaign)	Leipzig (Germany)	5 May to 5 June 2009
ALI09 [2 lidar systems] (Alomar Lidar Intercomparison campaign)	Alomar (Norway)	21 October to 5 November 2009
SOLI10 [2 lidar systems] (SOfia Lidar Intercomparison campaign)	Sofia (Bulgaria)	9 to 14 October 2010
ROLI10 [6 lidar systems] (ROmanian Lidar Intercomparison campaign)	Bucharest (Romania)	17 to 23 October 2010
SPALI10 [5 lidar systems] (SPAin Lidar Intercomparison campaign)	Madrid (Spain)	18 October to 5 November 2010

The intercomparison measurement campaigns allowed to compare the performances of many lidar systems, to define a standard methodology to be applied in the lidar system intercomparison, to

confirm the possibility to obtain reliable and homogeneous data within EARLINET, but also to understand the reasons of the possible failures and to individuate the way to solve them.

Further intercomparison measurement campaigns were planned in the period from January 2011 to June 2012 (Napoli, Lecce and L'Aquila EARLINET stations), but these have been shifted because main upgrades of the lidar systems are still in progress. Those inter-comparisons will be performed as soon as the major upgrades of the systems will be completed.

In the period March – December 2011, the work has been concentrated on the analysis of the data from the performed campaigns.

In order to perform the comparison among the optical products, the first step is to analyse the results of the QA tests for each single instrument. In fact, during the measurement campaigns, before the start of each measurement session, the participants were asked to perform a set of tests in order to check the quality of the performances for each single instrument. Two tests have been taken basically into account for this analysis: the Rayleigh fit test and the Telecover test, because these are considered as routine tests to be performed systematically on the instruments to check the optical alignment. Other tests were already performed independently in order to measure fixed instrumental parameters (Trigger delay, First range bin, Pulse Generator Test).

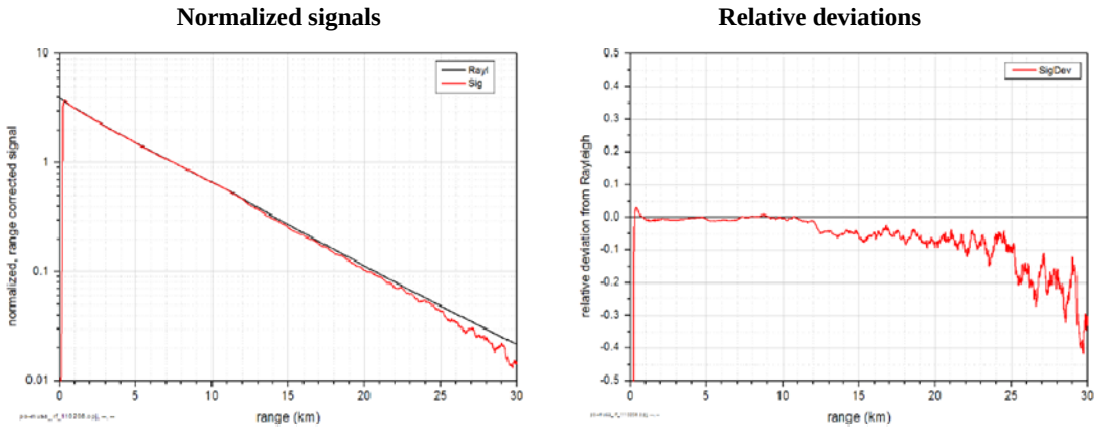

Figure 43. Example of Rayleigh fit test applied to lidar data at 387nm during EARLI09: range corrected lidar signal compared with the calculated clear air Rayleigh signal (left) and the relative deviation (right).

The Rayleigh fit test checks the quality of the lidar signals in the far range, where especially analog signals show distortions. The test is based on the fit of the far range lidar signal, assuming clear air in the upper troposphere, to the calculated clear air Rayleigh signal. In Figure 43, an example of result from the analysis of the Rayleigh fit test during EARLI09 is reported. From the relative deviations analysis on the right panel, it is evident that the test is excellent up to 12km of height with a deviation within 10% up to 25km. These are the typical conditions that must be fulfilled by a system acceptable for the intercomparison.

The Telecover test is based on the comparison of lidar signals from different parts of the telescope aperture and aims to test/verify the alignment of laser and optics. This test has to be performed for each single channel of a specific lidar system. In Figure 44, an example of analysis of the Telecover test measurements performed during EARLI09 for a single channel (532 nm) is showed. On the left panel, it is evident that the lines of different colors, corresponding to different parts of the telescope aperture, are overlapped. This means that all these parts of the telescope work well, as demonstrated also by the relative deviation respect to the mean, plotted in the right panel.

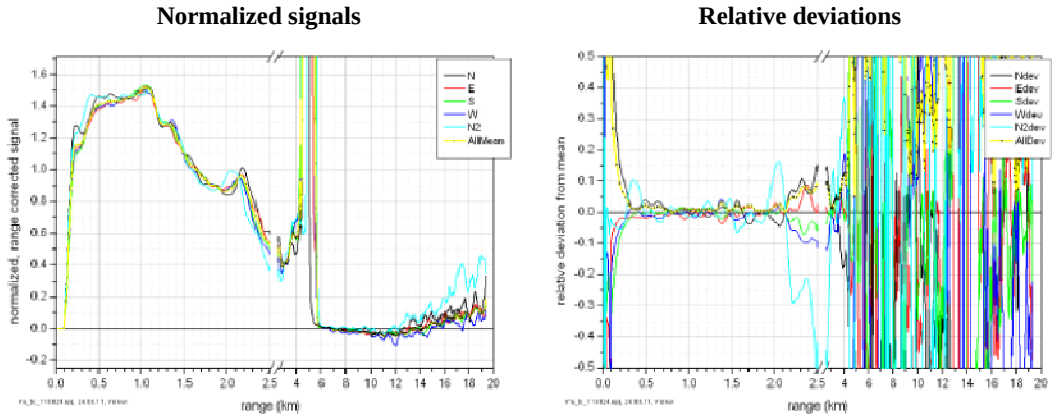

Figure 44. Example of Telecover test at 532nm during EARLI09. The different lines refer to the different parts of the telescope aperture. Range corrected lidar signals (left) and the corresponding relative deviations from the mean (right)

All the QA tests have been applied during the measurement campaigns for each single lidar instrument and have been used in order to solve specific problems before the actual intercomparison.

The second part of the analysis has been addressed to the comparison of the raw lidar signals and of the retrieved optical products (vertical profiles backscatter and extinction coefficients). We have selected for the analysis only the measurements where the QA tests were performed successfully. This selection has been done taking into account the measurement time intervals common for the participating lidar instruments and the uniformity of atmospheric conditions. In Figure 45, an example of the time distribution of the measurements of several instruments during a session (left panel) of EARLI09 is showed, together with an example of the corresponding temporal evolution of range corrected signals and time windows selected (right panel) for the analysis.

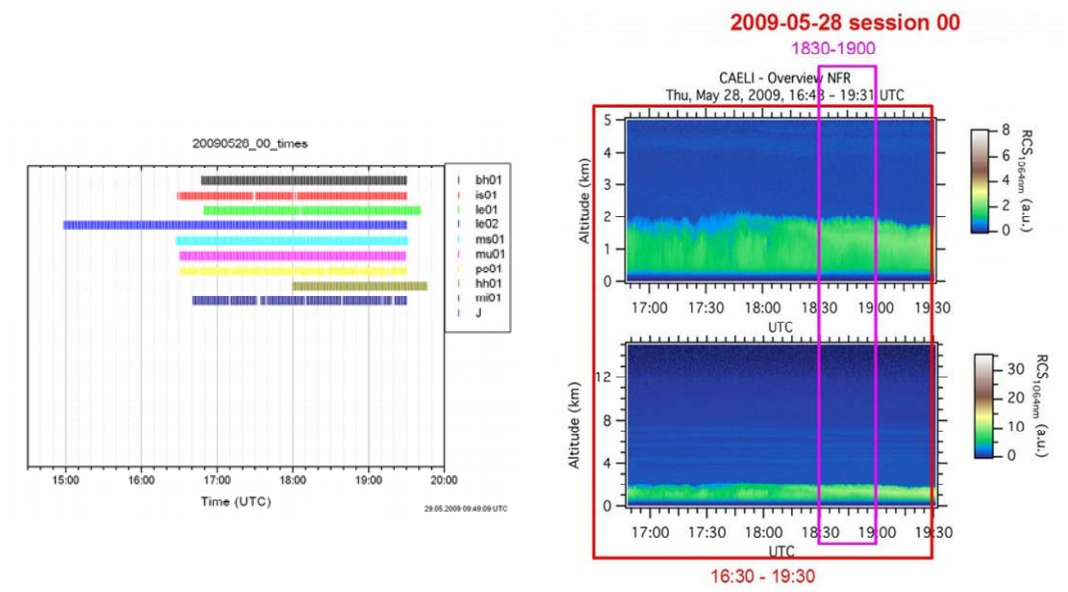

Figure 45. Example of measurement session with the indication of the measurement time period for each instrument (left panel) and the corresponding temporal evolution of the range corrected lidar signal at 1064 nm (right panel) with some time intervals selected for analysis (magenta and red boxes).

In the data analysis, it is crucial to take into account that data come from different instruments used by individual groups. Differences exist for the wavelengths used, acquisition mode (analog and/or photoncounting), space resolution, detection systems. All these factors were already taken into account in the data pre-processing performed by the Single Calculus Chain. Also for the optical data retrieval it is used the Single Calculus Chain, not only because it is the calculus module to retrieve the optical properties to be used throughout EARLINET, but also because the use of the SCC assures the uniformity of the data processing for all the instruments.

Examples of comparison of optical data from EARLI09 and SPALI10 are reported in the following. An example of comparison of backscatter coefficients at 1064nm for six lidar instruments, performed during EARLI09, are reported in Figure 46. The agreement among the different lidar instruments is satisfactory taking into account the different overlap.

An example of comparison of backscatter coefficient at 532nm, for three lidar instruments performed during SPALI10, is reported in Figure 47. Also in this case, the results can be considered satisfactory, with the only exception of low altitudes because of the different overlap functions of the lidar systems. A complete analysis of all the suitable comparisons performed during the measurement campaigns and the study of the relative deviations is in progress.

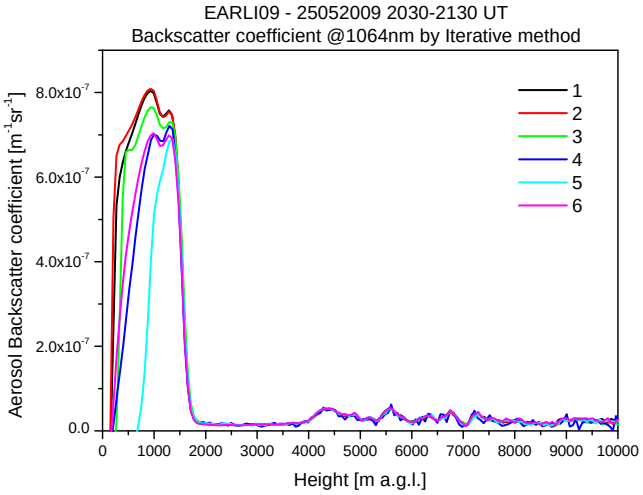

Figure 46. Comparison of backscatter coefficients profiles at 1064nm during EARLI09.

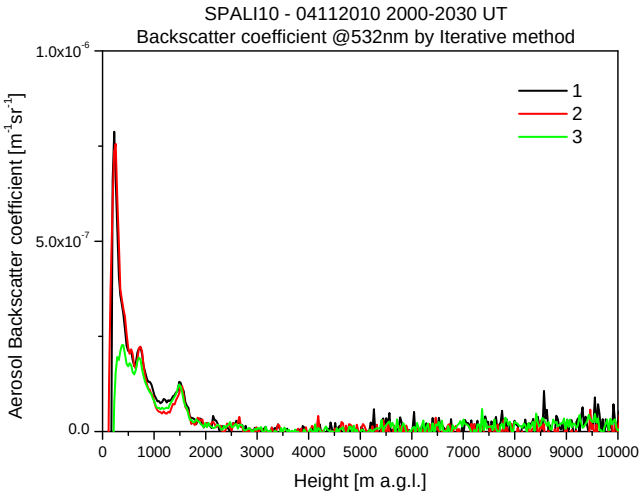

Figure 47. Comparison of backscatter coefficients profiles at 532 nm during SPALI10.

4 Activities planned for 2012

4.1 Dobson/Brewer team

The focus in the final phase of the project is on the Dobson-Brewer comparison during the Arosa campaign in July 2012 as another location with different atmospheric condition. Until now the campaigns in Sodankylä represents High Latitudes with high ozone vakues and in El Arenosillo Lower Latitudes at sea level with lower ozone values. Now Arosa stays for Midlatitudes at a high altitude with ordinary total ozone columns.

In addition another Langley campaign at Izaña on Tenerife is to confirm the findings of the last similar campaigns, hopefully this time with the participation of one of the WDCC Dobsons.

As especially the activities in 2011 suffered from the international financial crisis – no WDCC participant during El Arenosillo – it is hoped that we will not face similar problems in 2012. It is planned to compensate potential cancellations of the participation of important partners, which are financially caused, by the use of the DWD budget for visiting scientists: The corresponding application for such funding will be prepared during the first weeks in 2012.

A very important date in 2012 will be the Quadrennial Ozone Symposium in Toronto in August. Here the results of the ESA CEOS project can be presented to a large community of ozone and atmosphere scientists working in different fields.

The most important actions, however, will hopefully be the introduction of the DMB absorption coefficients and the successful reprocessing of the Dobson and Brewer data.

4.2 UV-Vis remote-sensing team

For the last part of the project, more work will be done to finalize and publish the CINDI NO2 profile intercomparison. Likewise, the intercomparison of aerosol profile retrieval methods will be continued. Another study has been recently initiated and will be further developed on stratospheric BrO column measurements, with as a main focus the harmonization and optimization of slant column retrievals. Lessons learned from the CINDI campaign will be summarized in preparation of a possible follow-up CINDI-2 campaign to be organized in 2013 or in 2014.

4.3 EARLINET team

During the last phase of the project the activities will focus on:

- Intercomparison campaigns: Napoli, Lecce and L'Aquila EARLINET stations (if the major upgrade of these systems, currently in progress, will be concluded)
- Complete data analysis from the performed intercomparison campaigns
- Preparation of the final report covering all the intercomparison campaigns
- Publication of the results of the lidar intercomparison campaigns in a scientific journal (probably AMT)

5 References

Aliwell, S. R., Van Roozendael, M., Johnston, P. V., Richter, A., Wagner, T. et al.: Analysis for BrO in zenith-sky spectra: An intercomparison exercise for analysis improvement, J. Geophys. Res., 107, D140, doi:10.1029/2001JD000329, 2002.

Bogumil, K., Orphal, J., Homann, T., Voigt, S., Spietz, P., Fleischmann, O. C., Vogel, A., Hartmann, M., Bovensmann, H., Frerik, J., and Burrows, J. P.: Measurements of molecular absorption spectra with the SCIAMACHY Pre-Flight Model: Instrument characterization and reference spectra for atmospheric remote sensing in the 230–2380 nm region, J. Photochem. Photobiol. A., 157, 167–184, 2003.

Bojkov, B. R., A. Redondas, A. Cede, E. Kyrö, R. Evans y T. McElroy: SAUNA – Sodankylä Total Ozone Intercomparison and Validation Campaign. Brewer/Dobson Summary, Proceedings of the Quadrennial Ozone Symposium, 2008.

Chance, K. V. and Spurr, R. J. D.: Ring effect studies: Rayleigh scattering, including molecular parameters for rotational Raman scattering, and the Fraunhofer spectrum, Appl. Optics, 36, 5224–5230, 1997.

Chance, K., and R.L. Kurucz: An improved high-resolution solar reference spectrum for Earth's atmosphere measurements in the ultraviolet, visible, and near infrared, http://www.cfa.harvard.edu/atmosphere, 2010.

Clémer, K., Van Roozendael, M., Fayt, C., Hendrick, F., Hermans, C., Pinardi, G., Spurr, R., Wang, P., and De Mazière, M.: Multiple wavelength retrieval of tropospheric aerosol optical properties from MAXDOAS measurements in Beijing, Atmos. Meas. Tech., 3, 863-878, doi:10.5194/amt-3-863-2010, 2010.

Daumont, M., Brion, J., Charbonnier, J., and Malicet, J.: Ozone UV spectroscopy, I: Absorption cross-sections at room temperature, J. Atmos. Chem., 15, 145–155, 1992.

Fioletov, V. E. et al., Performance of the ground-based total ozone network assessed using satellite data, J. Geophys. Res., 2008.

Fioletov, V., J. Kerr, C. Mcelroy, D. Wardle, V. Savastiouk, y T. Grajnar , The Brewer reference triad, Geophysical Research Letters, 32, 20805, 20805, 2005.

Fleischmann, O. C., Hartmann, M., Burrows, J. P., and Orphal, J.: New ultraviolet absorption cross-sections of BrO at atmospheric temperatures measured by time-windowing Fourier transform spectroscopy, J. Photochem. Photobiol. A, 168, 117–132, 2004.

Fraser, A., Adams, C., Drummond, J.R., Goutail, F., Manney, G., and Strong, K.: The Polar Environment Atmospheric Research Laboratory UV-Visible Ground-Based Spectrometer: First Measurements of O3, NO2, BrO, and OClO Columns. J. Quant. Spectrosc. Radiat. Transfer, 110 (12), 986-1004, doi.10.1016/j.jqsrt.2009.02.034, 2009.

Fried, A., Cantrell, C., Olson, J., Crawford, J. H., Weibring, P., Walega, J., Richter, D., Junkermann, W., Volkamer, R., Sinreich, R., Heikes, B. G., et al.: Detailed comparisons of airborne formaldehyde measurements with box models during the 2006 INTEX-B and MILAGRO campaigns: potential evidence for significant impacts of unmeasured and multi-generation

volatile organic carbon compounds, Atmos. Chem. Phys., 11, 11867-11894, doi:10.5194/acp-11-11867-2011, http://www.atmos-chem-phys.net/11/11867/2011, 2011.

Hak, C., Pundt, I., Trick, S., Kern, C., Platt, U., Dommen, J., Ordonez, C., Prévôt, A. S. H., Junkermann,W., Astorga-Lloréns, C., Larsen, B., Mellqvist, J., Strandberg, A., Yu, Y., Galle, B., Kleffmann, J., L¨orzer, J. C., Braathen, G. O., and Volkamer, R.: Intercomparison of four different in-situ techniques for ambient formaldehyde measurements in urban air, Atmos. Chem. Phys., 5, 2881–2900, http://www.atmos-chem-phys.net/5/2881/2005, 2005.

Heckel, A., Richter, A., Tarsu, T., Wittrock, F., Hak, C., Pundt, I., Junkermann,W., and Burrows, J. P.: MAX-DOAS measurements of formaldehyde in the Po-Valley, Atmos. Chem. Phys., 5, 909–918, http://www.atmos-chem-phys.net/5/909/2005, 2005.

Herman, J., A. Cede, E. Spinei, G. Mount, M. Tzortziou, and N. Abuhassan: NO2 column amounts from ground-based Pandora and MFDOAS spectrometers using the direct-sun DOAS technique: Intercomparisons and application to OMI validation, J. Geophys. Res., 114 (D13307), 10.1029/2009JD011848, 2009.

Hermans, C., A.C. Vandaele, S. Fally, M. Carleer, R. Colin, B. Coquart, A. Jenouvrier, M.-F. Mérienne: Absorption cross-section of the collision-induced bands of oxygen from the UV to the NIR, in: Proceedings of the NATO Advanced Research Workshop, Weakly Interacting Molecular Pairs: Unconventional Absorbers of Radiation in the Atmosphere, Fontevraud, France, 24 April-2May 2002, eds C. Camy-Peyret and A.A. Vigasin, Kluwer Academic Publishers, Boston, NATO Science Series IV Earth and Environmental Sciences, vol 27, pp 193-202, 2003.

Irie, H., Takashima, H., Kanaya, Y., Boersma, K. F., Gast, L., Wittrock, F., Brunner, D., Zhou, Y., and Van Roozendael, M.: Eight-component retrievals from ground-based MAX-DOAS observations, Atmos. Meas. Tech.., 4, 1027-1044 doi:10.5194/amt-4-1027-2011, 2011.

Malicet, J., Daumont, D., Charbonnier, J., Parisse, C., Chakir, A., and Brion, J.: Ozone UV spectroscopy. II. Absorption crosssections and temperature dependence, J. Atmos. Chem., 21, 263–273, 1995.

Meller, R. and Moortgat, G. K.: Temperature dependence of the absorption cross sections of formaldehyde between 223 and 323K in the wavelength range 225–375 nm, J. Geophys. Res., 105, 7089–7101, 2000.

Piters, A. J. M., Boersma, K. F., Kroon, M., Hains, J. C., Van Roozendael, M., Wittrock, F., Abuhassan, N., Adams, C., Akrami, M., Allaart, M. A. F., Apituley, A., Beirle, S., Bergwerff, J. B., Berkhout, A. J. C., Brunner, D., Cede, A., Chong, J., Clémer, K., Fayt, C., Frieß, U., Gast, L. F. L., Gil-Ojeda, M., Goutail, F., Graves, R., Griesfeller, A., Großmann, K., Hemerijckx, G., Hendrick, F., Henzing, B., Herman, J., Hermans, C., Hoexum, M., van der Hoff, G. R., Irie, H., Johnston, P. V., Kanaya, Y., Kim, Y. J., Klein Baltink, H., Kreher, K., de Leeuw, G., Leigh, R., Merlaud, A., Moerman, M. M., Monks, P. S., Mount, G. H., Navarro-Comas, M., Oetjen, H., Pazmino, A., Perez-Camacho, M., Peters, E., du Piesanie, A., Pinardi, G., Puentedura, O., Richter, A., Roscoe, H. K., Schönhardt, A., Schwarzenbach, B., Shaiganfar, R., Sluis, W., Spinei, E., Stolk, A. P., Strong, K., Swart, D. P. J., Takashima, H., Vlemmix, T., Vrekoussis, M., Wagner, T., Whyte, C., Wilson, K. M., Yela, M., Yilmaz, S., Zieger, P., and Zhou, Y.: The Cabauw Intercomparison campaign for Nitrogen Dioxide measuring Instruments (CINDI): design, execution, and early results, Atmos. Meas. Tech., 5, 457-485, doi:10.5194/amt-5-457-2012, 2012.

Rodgers, C.D., Characterization and error analysis of profiles derived from remote sensing measurements, J. Geophys. Res., 95, 5587-5595, 1990.

Roscoe, H.K, M. Van Roozendael, C. Fayt, A. du Piesanie, N. Abuhassan, C. Adams, M. Akrami, A. Cede, J. Chong, K. Clemer, U. Friess, M. Gil Ojeda, F. Goutail, R. Graves, A. Griesfeller, K. Grossmann, G. Hemerijckx, F. Hendrick, J. Herman, C. Hermans, H. Irie, P.V. Johnston, Y. Kanaya, K. Kreher, R. Leigh, A. Merlaud, G.H. Mount, M. Navarro, H. Oetjen, A. Pazmino, M. Perez-Camacho, E. Peters, G. Pinardi, O. Puentedura, A. Richter, A. Schoenhardt, R. Shaiganfar, E. Spinei, K. Strong, H. Takashima, T. Vlemmix, M. Vrekoussis, T. Wagner, F. Wittrock, M. Yela, S. Yilmaz, F. Boersma, J. Hains, M. Kroon, A. Piters, Y.J. Kim: Intercomparison of slant column measurements of NO_2 and O_4 by MaxDOAS and zenith-sky UV and visible spectrometers, Atm. Meas. Tech. 3, 1629-1646, 2010.

Shaiganfar, R., S. Beirle, M. Sharma, A. Chauhan, R.P. Singh, T. Wagner: Estimation of NOx emissions from Delhi using Car MAX-DOAS observations and comparison with OMI satellite data, Atmos. Chem. Phys., 11, 10871-10887, 2011.

Vandaele, A. C., Hermans, C., Simon, P. C., Van Roozendael, M., Guilmot, J. M., Carleer, M., and Colin, R.: Fourier transform measurement of NO_2 absorption cross-section in the visible range at room temperature, J. Atmos. Chem., 25, 289–305, 1996.

Wagner, T., Dix, B., Friedeburg, C. v., Frieß, U., Sanghavi, S., Sinreich, R., and Platt, U.: MAX-DOAS O_4 measurements – a new technique to derive information on atmospheric aerosols. (I) Principles and information content, J. Geophys. Res., 109, doi:10.1029/2004JD004904, 2004.

Wittrock, F., Oetjen, H., Richter, A., Fietkau, S., Medeke, T., Rozanov, A., and Burrows, J.P.: MAX-DOAS measurements of atmospheric trace gases in Ny-Alesund – Radiative transfer studies and their application, Atmos. Chem. Phys., 4, 955–966, doi:10.5194/acp-4-955-2004, 2004.